1970ApJ...162..217L

THE ASTROPHYSICAL JOURNAL, 162:217–238, October 1970
© 1970. The University of Chicago All rights reserved. Printed in U.S.A.

# PHOTOMETRY OF HIGH-LUMINOSITY M-TYPE STARS

THOMAS A. LEE*
NASA-Goddard Institute for Space Studies, New York, New York, and
Lunar and Planetary Laboratory, University of Arizona, Tucson

*Received 1970 March 30; revised 1970 May 11*

## ABSTRACT

Photometric observations extending to 3.4 $\mu$ are presented for a sample of high-luminosity M stars. Intrinsic properties (color indices, effective temperatures, bolometric corrections) are determined for giants and supergiants; the supergiants are redder than the giants and have slightly lower effective temperatures. A weak luminosity distinction among the supergiants is seen in the infrared color data. The mean law of interstellar extinction, derived from the colors of distant reddened M supergiants, yields $R = 3.6 \pm 0.3$ (for M stars), and no large-scale anomalous regions are found. The extreme Population I character of M supergiants is confirmed by their spatial distribution. They are highly concentrated to the galactic plane and suggest the same spiral structure shown by other early-type objects. The Ia supergiants show the strongest concentration in the plane—equal to that of the O and B stars.

## I. INTRODUCTION

Recent advances in infrared instrumentation and observing techniques have led to numerous discoveries of new and fascinating infrared sources. The potential rewards from investigations of other more common types of stars in the near- and intermediate-infrared, however, are also great. The M-type supergiants, for example, are ideally suited to such a study. These stars are located primarily in the galactic plane, and because of their intrinsic redness and high luminosity they can be observed at great distances in the infrared where the interstellar extinction is reduced. Recent theoretical investigations of M supergiants, the majority of which are thought to represent an advanced evolutionary stage of a highly massive star, include the construction of models for the carbon-burning and later phases leading to supernovae (Hayashi and Cameron 1962; Hayashi, Hōshi, and Sugimoto 1962; Sugimoto *et al.* 1968; Stothers and Chin 1969) as well as the possible effects of energy losses by neutrinos (Hayashi *et al.* 1962; Sugimoto *et al.* 1968; Stothers and Chin 1969). However, Stothers and Chin (1968) find that the inclusion of bound-free absorption in the opacity and semiconvective mixing in the stellar intermediate zone results in an earlier red-supergiant phase during core helium burning. Stothers (1969) also finds that the relative numbers of red and blue supergiants in clusters and associations require the existence of neutrino emission for phases of evolution beyond core helium burning. In spite of very complex problems due to blanketing corrections and the equation of state, preliminary stellar atmospheres of M supergiants have been calculated by Tsuji (1966), Gingerich *et al.* (1966), and Gingerich and Kumar (1964). Due to an opacity minimum and Planck distribution maximum, the 3000° K models show evidence for a continuum peak near 1.6 $\mu$, a feature which is positively correlated with luminosity.

Since M supergiants are stars of the extreme Population I type, they are very important for studies of galactic structure. Sharpless (1966) finds that most M supergiants are located in or near O associations, while Humphreys (1969) obtains good agreement regarding kinematics and spatial distribution for the M supergiants and other Population I stars in Perseus. Moreover, Walker's (1967) dye-transfer photography reveals that the M supergiants are good tracers of spiral structure in M33. Therefore, extensive studies of these stars in our Galaxy may disclose distant spiral features similar to those shown by H I and other tracers.

* NRC-NASA Resident Research Associate.



© American Astronomical Society • Provided by the NASA Astrophysics Data System

1970ApJ...162..217L



The purpose of the present investigation is threefold: (*a*) to determine the intrinsic properties of M supergiants (intrinsic colors, bolometric corrections, etc.), (*b*) to study the quantity and wavelength dependence of interstellar extinction for distant objects in the galactic plane, and (*c*) to determine how successfully the M supergiants reveal the distant morphology of our Galaxy.

## II. THE OBSERVATIONS

The observations, which consist of wide-band photoelectric photometry extending from the ultraviolet to 3.4 $\mu$ in the infrared, were obtained at the Catalina Observatory of the Lunar and Planetary Laboratory of the University of Arizona. The stars were selected from the Case surveys of reddened M-type stars in the galactic plane (Nassau, Blanco, and Morgan 1954; Blanco and Nassau 1957). All the BD stars found in these surveys, a large fraction of which are known to be supergiants (Sharpless 1966), are included in the present study as well as some of the fainter non-BD stars. The brighter M supergiants were also observed (excluding those in Perseus studied by Johnson and Mendoza V. [1966]), so that the data, presented in Table 1, are reasonably complete in the galactic plane ($l^{II} = 0°$–$240°$) to $V = 9.0$ mag.

---

*Column (1), star identification.*—Either BD or Case numbers are given.

*Column (2), spectral and luminosity type.*—The types were taken from the following sources: Bidelman (1951, 1954, 1957); Bidelman and Stephenson (1956); Blanco and Nassau (1957); Cowley (1969); Gahm and Zappala (1969); Hoffleit (1964); Humphreys (1969); Johnson *et al.* (1966); Keenan (1942, 1963); McCuskey (1967); Nassau *et al.* (1954); Sharpless (1956, 1958, 1966); Wawrukiewicz (1970); and Yamashita (1967). In those instances when differing spectral types were assigned to the same star, a mean type was adopted. The recent results of Wawrukiewicz (1970), based on narrow-band photometry of the TiO band near 7050 Å, have been given high weight in this regard. Several stars having blue companions are readily identified as such from their $U - B$ colors; most of these supergiants are recognized variables of the VV Cephei type (Bidelman 1954; Cowley 1969). Those luminosity classes enclosed in parentheses were not determined spectroscopically but are estimates made from the distance modulus and the amount of interstellar extinction (see § IV*c*).

*Columns (3) and (4), galactic coordinates.*

*Columns (5)–(13), observed magnitude and colors.*—The observations are on the wide-band *UBVRIJHKL* system of Johnson *et al.* (1966) and extend from 0.36 to 3.4 $\mu$. The filters and their effective wavelengths are as follows: $U$(0.36 $\mu$), $B$(0.44 $\mu$), $V$(0.55 $\mu$), $R$(0.70 $\mu$), $I$(0.90 $\mu$), $J$(1.25 $\mu$), $H$(1.62 $\mu$), $K$(2.2 $\mu$), and $L$(3.4 $\mu$).

*Column (14), number of observations.*—The two numbers refer to the number of independent *UBVRI* and *JHKL* measurements.

*Column (15), remarks.*—Asterisk indicates note, as noted in Notes to Table 2.

© American Astronomical Society • Provided by the NASA Astrophysics Data System

TABLE 1

Reddened Supergiants and Giants

| Star | Spectrum | $l^{II}$ | $b^{II}$ | V | U-V | B-V | V-R | V-I | V-J | V-H | V-K | V-L | N | R |
|---|---|---|---|---|---|---|---|---|---|---|---|---|---|---|
| -27°12032 | M3.0 Ia | 01°.5 | -0°.7 | 9.66 | 5.0 | 2.84 | 3.12 | 5.43 | 6.54 | 7.67 | 8.12 | 8.75 | 3-3 | * |
| -22°4575 | S | 08.3 | -0.9 | 6.52 | 5.2 | 2.89 | 2.62 | 4.41 | 5.29 | 6.39 | 7.02 | 8.13 | 3-3 | * |
| -21°4897 | M4.0 (I) | 09.8 | -1.0 | 9.78 | 3.6 | 2.39 | 2.71 | 4.77 | 6.00 | 7.28 | 7.75 | 8.13 | 3-4 | |
| -20°5056 | M2.5 (I) | 10.3 | -1.2 | 11.21 | - | 2.81 | 2.92 | 5.12 | 6.32 | 7.59 | 8.03 | 8.50 | 3-3 | |
| -19°4907 | M2.5 Ib | 11.6 | -0.7 | 9.40 | 4.0 | 2.06 | 1.96 | 3.46 | 4.46 | 5.53 | 5.80 | 6.04 | 3-3 | |
| -19°5039 | M3 (III) | 13.3 | -4.1 | 9.06 | 3.8 | 1.88 | 1.82 | 3.22 | 4.10 | 5.11 | 5.37 | 5.58 | 2-3 | |
| Case 49 | M2.0 Iab | 17.8 | -0.6 | 11.03 | 6.3 | 3.06 | 3.08 | 5.36 | 6.69 | 8.03 | 8.53 | 9.02 | 2-3 | |
| -14°5105 | M2.0 Iab | 18.3 | -2.4 | 7.85 | 4.50 | 2.26 | 2.06 | 3.70 | 4.77 | 5.79 | 6.14 | 6.53 | 3-3 | |
| Case 48 | M2.5 Iab+B | 18.4 | +0.3 | 10.41 | 2.16 | 1.74 | 2.54 | 4.81 | 6.27 | 7.66 | 8.19 | 8.60 | 3-3 | * |
| -12°5055 | M4.0 Ia-ab | 19.1 | -0.4 | 10.09 | 4.8 | 2.84 | 3.49 | 6.07 | 7.37 | 8.56 | 9.11 | 9.81 | 3-5 | * |
| -10°4738 | M3.0 (I) | 22.4 | -1.5 | 9.55 | 4.5 | 2.31 | 2.41 | 4.31 | 5.33 | 6.45 | 6.79 | 7.11 | 2-4 | |
| -08°4645 | M3.5 (I) | 23.2 | -0.6 | 10.38 | 5.2 | 2.51 | 2.70 | 4.80 | 5.99 | 7.20 | 7.60 | 7.90 | 2-4 | |
| -06°4827 | M0 (I)+B | 25.7 | -0.4 | 10.46 | 2.47 | 1.89 | 2.48 | 4.43 | 5.66 | 6.94 | 7.35 | 7.75 | 3-4 | |
| -05°4743 | M2.0 (I) | 27.6 | -0.6 | 10.20 | 4.6 | 2.28 | 2.22 | 3.96 | 4.99 | 6.07 | 6.41 | 6.72 | 3-5 | |
| + 0°4030 | M1 (I) | 33.5 | +0.5 | 10.44 | 4.9 | 2.48 | 2.30 | 4.09 | 5.17 | 6.34 | 6.66 | 6.94 | 3-4 | |
| + 0°4064 | M1.5 Iab | 34.0 | -1.2 | 8.87 | 4.7 | 2.58 | 2.38 | 4.21 | 5.36 | 6.48 | 6.85 | 7.23 | 4-4 | * |
| Case 55 | M0 Ia | 38.6 | +0.7 | 10.57 | 5.3 | 3.19 | 3.07 | 5.32 | 6.66 | 8.06 | 8.59 | 9.03 | 3-3 | * |
| +10°3721 | M5 III | 42.7 | +4.1 | 7.40 | 3.26 | 1.75 | 2.29 | 4.24 | 5.19 | 6.22 | 6.49 | 6.75 | 4-4 | * |
| +09°3920 | M2.0 (III) | 43.2 | +3.1 | 9.36 | 4.01 | 1.84 | 1.63 | 2.95 | 3.75 | 4.72 | 4.95 | 5.17 | 2-3 | |
| +12°3703 | M2.5 (III) | 44.7 | +5.2 | 9.10 | 3.77 | 1.76 | 1.55 | 2.85 | 3.66 | 4.57 | 4.80 | 4.99 | 3-4 | |
| +22°3840 | M2: (I)+B | 59.7 | -2.5 | 7.76 | 1.20 | 0.92 | 2.69 | 5.43 | 6.91 | 7.93 | 8.30 | 8.67 | 6-7 | * |
| +24°3902 | M1.5 Ia | 61.6 | -0.7 | 9.30 | 5.6 | 3.03 | 2.70 | 4.81 | 6.20 | 7.19 | 7.70 | 8.30 | 4-4 | |
| +25°4097 | M2.0 II | 64.0 | -3.3 | 7.99 | 4.48 | 2.27 | 2.16 | 3.93 | 4.93 | 5.97 | 6.32 | 6.63 | 5-5 | * |
| +29°3730 | M4.0 III | 65.8 | +2.8 | 7.62 | 3.33 | 1.70 | 1.93 | 3.63 | 4.54 | 5.41 | 5.68 | 5.95 | 4-5 | * |
| Case 61 | M1.5 Iab | 67.9 | +0.3 | 10.07 | 5.2 | 2.65 | 2.47 | 4.34 | 5.49 | 6.63 | 7.05 | 7.56 | 3-3 | * |
| Case 62 | M2.5 (I)+B | 67.9 | +0.3 | 10.29 | 3.9 | 2.38 | 2.39 | 4.27 | 5.49 | 6.58 | 7.05 | 7.71 | 3-3 | |
| +35°4077 | M1.5 Iab | 74.2 | -0.6 | 9.72 | 5.0 | 2.93 | 2.89 | 5.07 | 6.42 | 7.61 | 8.11 | 8.60 | 3-4 | |
| +35°4138 | M3.0 (III) | 75.0 | -1.9 | 9.18 | 3.93 | 1.82 | 1.74 | 3.24 | 4.07 | 5.02 | 5.31 | 5.56 | 2-3 | |
| +36°4025 | M3.0 Iab | 75.3 | +0.2 | 9.33 | 5.5 | 3.01 | 3.20 | 5.69 | 6.98 | 8.18 | 8.75 | 9.31 | 4-4 | * |
| Case 68 | S | 75.7 | -1.0 | 10.20 | 4.0 | 2.18 | 3.38 | 5.76 | 6.90 | 8.01 | 8.41 | 8.79 | 3-3 | * |
| +37°3903 | M3.5 Ia | 75.8 | +0.4 | 9.97 | 6.4 | 3.26 | 3.75 | 6.53 | 7.94 | 9.21 | 9.80 | 10.41 | 3-4 | * |
| Case 66 | M3.5 Ia | 77.0 | +0.2 | 11.14 | 6.3 | 3.49 | 4.25 | 7.13 | 8.79 | 10.29 | 10.97 | 11.60 | 3-3 | * |



© American Astronomical Society • Provided by the NASA Astrophysics Data System

TABLE 1 (continued)

| Star | Spectrum | $l^{II}$ | $b^{II}$ | V | U-V | B-V | V-R | V-I | V-J | V-H | V-K | V-L | N | R |
|---|---|---|---|---|---|---|---|---|---|---|---|---|---|---|
| +39°4208 | M2.0 Ia-ab | 78.6 | +0.7 | 8.13 | 5.3 | 2.88 | 2.68 | 4.75 | 6.02 | 7.19 | 7.68 | 8.21 | 5-6 | * |
| +43°3477 | M0 (I) | 79.1 | +6.3 | 10.11 | 4.7 | 2.49 | 2.21 | 3.91 | 5.09 | 6.21 | 6.62 | 7.01 | 3-4 | |
| +45°3349 | M3: Ia | 87.1 | +0.5 | 8.85 | 5.1 | 2.56 | 2.75 | 4.94 | 6.16 | 7.16 | 7.63 | 8.15 | 3-3 | * |
| +58°2249 | M1ep Ib+B | 98.2 | +6.3 | 5.75 | 1.34 | 1.34 | 1.50 | 2.83 | 3.83 | 4.73 | 5.00 | 5.26 | 3-4 | |
| +58°2316 | M2.0 Ia | 100.6 | +4.3 | 4.17 | 4.71 | 2.26 | 2.10 | 3.86 | 4.69 | 5.47 | 5.82 | 6.26 | 3-3 | * |
| +61°2134 | M3.5 Ia-ab | 101.5 | +8.5 | 8.88 | 4.6 | 2.36 | 2.53 | 4.59 | 5.62 | 6.66 | 7.08 | 7.55 | 2-3 | * |
| +55°2737 | K5: Ia-0 | 103.2 | -1.1 | 6.65 | 4.60 | 2.22 | 1.71 | 2.87 | 3.82 | 4.43 | 4.78 | 5.19 | 3-3 | * |
| +58°2396 | M2.0 Ia | 103.7 | +3.0 | 10.03 | 5.0 | 2.67 | 2.49 | 4.53 | 5.90 | 7.02 | 7.50 | 7.98 | 2-3 | * |
| +56°2793 | M2: Ib | 104.6 | -0.8 | 8.09 | 4.6 | 2.28 | 2.20 | 3.95 | 5.12 | 5.96 | 6.31 | 6.74 | 3-3 | * |
| +62°2007 | M2ep Ia+0 | 104.9 | +7.0 | 5.16 | 2.06 | 1.72 | 1.75 | 3.20 | 4.08 | 4.95 | 5.27 | 5.60 | 2-3 | * |
| +54°2863 | M4 Iab+B: | 105.8 | -3.5 | 8.70 | 3.8 | 2.34 | 2.44 | 4.40 | 5.80 | 6.57 | 7.13 | 7.93 | 3-3 | * |
| Case 75 | M3.5 Ia | 105.9 | +0.6 | 11.74 | - | 3.12 | 3.46 | 6.06 | 7.72 | 9.15 | 9.81 | 10.42 | 3-3 | |
| +59°2541 | M2.5 (III) | 106.9 | +2.1 | 9.96 | 4.2 | 2.01 | 1.82 | 3.31 | 4.24 | 5.28 | 5.56 | 5.88 | 3-3 | |
| Case 78 | M1.5 Ib | 107.9 | 0.0 | 10.92 | 5.6 | 2.90 | 2.85 | 5.08 | 6.48 | 7.77 | 8.30 | 8.80 | 3-3 | |
| Case 79 | S | 109.3 | +1.6 | 11.03 | 5.4 | 2.90 | 3.18 | 5.66 | 7.06 | 8.35 | 9.00 | 9.73 | 3-3 | |
| Case 81 | M2.0 Iab | 111.2 | -0.1 | 10.02 | 5.2 | 2.65 | 2.45 | 4.27 | 5.55 | 6.72 | 7.17 | 7.63 | 3-3 | |
| +57°2750 | M2.5 Ia | 112.3 | -3.2 | 9.51 | 5.0 | 2.72 | 2.70 | 4.75 | 5.92 | 7.04 | 7.56 | 8.13 | 4-4 | * |
| +60°2613 | M3.5 Ia+(B) | 115.0 | -0.1 | 8.90 | 3.9 | 2.58 | 2.82 | 5.00 | 6.48 | 7.37 | 7.88 | 8.51 | 4-2 | * |
| +60°2634 | M2.5 Iab | 115.9 | -1.0 | 9.17 | 5.0 | 2.51 | 2.54 | 4.55 | 5.83 | 6.86 | 7.29 | 7.80 | 3-3 | * |
| +64°1842 | M2.0 II | 115.9 | +3.7 | 9.75 | 5.0 | 2.46 | 2.24 | 4.09 | 5.13 | 6.27 | 6.66 | 6.99 | 3-3 | |
| +63°2073 | M0 Ib | 116.8 | +2.1 | 10.15 | 4.7 | 2.39 | 2.05 | 3.65 | 4.74 | 5.81 | 6.17 | 6.49 | 3-3 | |
| +61° 08 | M1ep Ib+B | 118.2 | +0.1 | 9.49 | 2.30 | 1.72 | 1.73 | 3.19 | 4.16 | 5.15 | 5.49 | 5.79 | 2-3 | * |
| Case 23 | M2.0 Iab | 122.8 | +1.9 | 10.82 | 5.4 | 2.74 | 2.68 | 4.75 | 6.00 | 7.37 | 7.90 | 8.30 | 3-2 | |
| +62° 207 | M3.5 Ia | 124.8 | +0.8 | 9.82 | 4.7 | 2.51 | 2.57 | 4.69 | 5.84 | 6.94 | 7.36 | 7.77 | 3-4 | * |
| +57° 258 | M1.5 Ib | 126.6 | -4.4 | 8.62 | 4.42 | 2.12 | 1.76 | 3.18 | 4.21 | 5.09 | 5.38 | 5.62 | 3-2 | |
| +59° 274 | M0.5 Iab-b | 128.1 | -1.7 | 8.48 | 4.17 | 2.06 | 1.68 | 3.06 | 3.98 | 4.85 | 5.17 | 5.44 | 2-3 | |
| +60° 310 | M0Ib+Be | 129.0 | -0.9 | 9.24 | 2.15 | 1.72 | 1.64 | 2.91 | 3.96 | 4.84 | 5.14 | 5.43 | 3-3 | * |
| +55° 388 | M3.0 Ib | 130.1 | -5.6 | 8.82 | 4.08 | 1.99 | 1.92 | 3.66 | 4.63 | 5.60 | 5.95 | 6.27 | 2-4 | |
| +54° 444 | M4.0 Ib+B | 133.1 | -6.2 | 8.26 | 3.46 | 2.10 | 2.18 | 4.01 | 5.20 | 6.05 | 6.43 | 7.07 | 3-3 | * |
| +58° 501 | M2.0 Iab | 136.3 | -0.5 | 9.37 | 5.3 | 2.71 | 2.57 | 4.61 | 5.84 | 6.99 | 7.42 | 7.86 | 4-3 | * |
| +57° 647 | M2.0 Ia | 138.3 | -1.4 | 9.38 | 5.4 | 2.73 | 2.55 | 4.62 | 5.81 | 6.91 | 7.36 | 7.82 | 5-4 | * |
| +59° 580 | M1 Ib | 138.3 | +1.1 | 9.91 | 5.0 | 2.32 | 1.97 | 3.53 | 4.68 | 5.71 | 6.05 | 6.27 | 3-2 | |
| +59° 594 | M1 Iab | 139.0 | +1.9 | 8.90 | 5.4 | 2.78 | 2.36 | 4.17 | 5.45 | 6.50 | 6.94 | 7.32 | 5-4 | * |
| Case 31 | M2.0 Ib | 139.2 | -1.3 | 9.88 | 4.9 | 2.70 | 2.63 | 4.62 | 5.87 | 7.09 | 7.54 | 8.05 | 3-3 | |
| Case 33 | M3.0 Iab | 141.3 | -2.3 | 10.65 | 4.7 | 3.09 | 3.36 | 5.80 | 7.30 | 8.64 | 9.29 | 10.06 | 5-4 | * |



© American Astronomical Society • Provided by the NASA Astrophysics Data System

TABLE 1 (continued)

| Star | Spectrum | $l^{II}$ | $b^{II}$ | V | U-V | B-V | V-R | V-I | V-J | V-H | V-K | V-L | N | R |
|---|---|---|---|---|---|---|---|---|---|---|---|---|---|---|
| +54° 651 | M0 Iab | 142.5 | -2.4 | 9.23 | 5.1 | 2.52 | 2.06 | 3.65 | 4.68 | 5.80 | 6.14 | 6.48 | 4-4 | |
| Case 34 | M3.5 Iab-b | 142.7 | -2.4 | 10.32 | 5.1 | 2.70 | 2.91 | 5.25 | 6.65 | 7.85 | 8.27 | 8.78 | 3-3 | |
| +55° 778 | M2.5 (III) | 143.2 | -0.2 | 9.98 | 4.8 | 2.15 | 1.97 | 3.60 | 4.55 | 5.62 | 5.93 | 6.19 | 3-3 | |
| +54° 739 | M2.0 III: | 148.7 | +2.4 | 10.10 | 6.0 | 2.70 | 2.61 | 4.65 | 5.83 | 7.06 | 7.51 | 7.76 | 3-3 | * |
| +44°1005 | M2.0 III | 160.0 | -1.1 | 10.24 | 4.8 | 2.36 | 2.22 | 3.98 | 5.06 | 6.14 | 6.48 | 6.71 | 4-4 | |
| +42°1065 | M0 (III) | 162.0 | -1.0 | 10.06 | 3.95 | 1.77 | 1.45 | 2.55 | 3.31 | 4.21 | 4.34 | 4.49 | 3-2 | |
| +43°1131 | M3.5 (III) | 162.3 | +0.1 | 7.43 | 3.80 | 1.76 | 1.70 | 3.22 | 4.04 | 4.97 | 5.23 | 5.43 | 3-2 | |
| +43°1183 | M2.0 (I) | 163.1 | +1.8 | 9.45 | 4.6 | 2.20 | 1.97 | 3.59 | 4.51 | 5.57 | 5.92 | 6.20 | 3-3 | |
| +39°1070 | M1.5 III | 164.3 | -3.2 | 9.82 | 4.32 | 2.03 | 1.68 | 3.02 | 3.82 | 4.83 | 5.11 | 5.34 | 2-3 | |
| Case 39 | M1 III | 164.6 | -2.6 | 10.39 | 4.2 | 2.08 | 1.88 | 3.35 | 4.17 | 5.31 | 5.58 | 5.85 | 3-3 | |
| +49°1488 | K5: Iab | 165.4 | +16.2 | 4.75 | 4.10 | 1.92 | 1.40 | 2.47 | 3.24 | 4.05 | 4.25 | 4.55 | 2-3 | * |
| +38°1162 | M1.5 (I) | 169.5 | +2.3 | 9.77 | 4.8 | 2.42 | 2.21 | 3.96 | 5.18 | 6.30 | 6.69 | 7.05 | 4-4 | * |
| +46°1271 | M5: S | 172.3 | +25.2 | 6.98 | 2.9 | 1.73 | 2.73 | 5.02 | 6.17 | 7.08 | 7.42 | 7.70 | 2-5 | * |
| +31°1049 | M1.5 Iab | 176.9 | +0.7 | 6.21 | 4.31 | 2.09 | 1.78 | 3.20 | 4.10 | 5.01 | 5.31 | 5.58 | 3-3 | |
| +32°1113 | M1 (III)+B | 177.7 | +3.0 | 9.16 | 2.72 | 1.53 | 1.37 | 2.42 | 3.19 | 4.13 | 4.36 | 4.63 | 3-3 | |
| +32°1109 | M2.5 III | 177.9 | +2.7 | 6.28 | 3.79 | 1.73 | 1.62 | 3.03 | 3.88 | 4.79 | 5.02 | 5.20 | 3-3 | |
| +28° 834 | M1.5 (I) | 179.0 | -1.4 | 9.89 | 4.5 | 2.15 | 1.92 | 3.44 | 4.38 | 5.43 | 5.76 | 6.04 | 2-2 | |
| +24°1072 | M1 III | 185.4 | +1.3 | 9.65 | 3.57 | 1.79 | 1.56 | 2.87 | 3.73 | 4.67 | 4.92 | 5.18 | 2-3 | |
| +25°1131 | M3.5 (III) | 185.5 | +2.7 | 7.55 | 3.48 | 1.64 | 1.55 | 2.96 | 3.78 | 4.69 | 4.93 | 5.10 | 2-4 | |
| +23°1138 | M1 (I) | 186.1 | -0.0 | 10.26 | 4.9 | 2.52 | 2.26 | 4.00 | 5.09 | 6.25 | 6.66 | 6.98 | 3-3 | |
| +18° 875 | M2.0 Ib | 187.2 | -8.1 | 4.33 | 4.30 | 2.08 | 1.78 | 3.21 | 4.02 | 4.93 | 5.23 | 5.59 | 5-9 | * |
| +23°1243 | M2ep Iab+B | 187.9 | +2.2 | 7.38 | 2.86 | 1.82 | 1.80 | 3.34 | 4.33 | 5.21 | 5.52 | 5.82 | 3-3 | * |
| +23°1240 | M0 (III) | 188.1 | +2.1 | 9.12 | 3.82 | 1.81 | 1.43 | 2.42 | 3.22 | 4.08 | 4.31 | 4.52 | 2-4 | |
| +22°1220 | M1 Ia | 188.2 | +2.2 | 6.39 | 4.72 | 2.24 | 1.84 | 3.32 | 4.16 | 5.11 | 5.41 | 5.77 | 3-3 | * |
| +21°1146 | M1 Iab | 189.1 | +1.6 | 6.56 | 4.02 | 2.25 | 1.91 | 3.39 | 4.36 | 5.36 | 5.62 | 6.02 | 5-4 | * |
| +19°1183 | M0 (III) | 190.1 | -1.4 | 9.08 | 3.39 | 1.71 | 1.29 | 2.28 | 2.95 | 3.77 | 3.98 | 4.16 | 2-3 | |
| +13°1110 | M1 III | 195.8 | -3.5 | 9.01 | 3.81 | 1.79 | 1.51 | 2.74 | 3.51 | 4.41 | 4.65 | 4.82 | 4-4 | |
| +13°1212 | M3.5 (I) | 197.1 | -0.3 | 10.44 | 4.7 | 2.53 | 2.64 | 4.63 | 5.72 | 6.85 | 7.26 | 7.78 | 2-2 | |
| +07°1055 | M2.0 Iab | 199.8 | -9.0 | 0.40 | 3.96 | 1.89 | 1.59 | 2.87 | 3.33 | 4.13 | 4.41 | 4.83 | 2-2 | * |
| +10°1085 | M4.0 (III) | 200.1 | -2.4 | 8.90 | 3.44 | 1.64 | 1.70 | 3.23 | 4.05 | 4.98 | 5.25 | 5.47 | 2-4 | |
| +05°1198 | M3.0 Iab | 204.3 | -4.2 | 8.04 | 3.88 | 1.92 | 1.94 | 3.58 | 4.53 | 5.52 | 5.83 | 6.09 | 2-3 | |
| +02°1451 | M1.5 (I) | 211.4 | +1.1 | 9.20 | 4.1 | 2.24 | 1.95 | 3.50 | 4.47 | 5.57 | 5.89 | 6.20 | 3-4 | |
| -09°1649 | M2.0 II | 221.3 | -5.4 | 9.72 | 3.68 | 1.66 | 1.53 | 2.74 | 3.46 | 4.35 | 4.60 | 4.75 | 2-3 | |
| -14°1971 | M2ep Iab+B | 230.6 | +2.5 | 4.98 | 1.76 | 1.47 | 1.56 | 2.89 | 3.73 | 4.64 | 4.87 | 5.15 | 2-4 | |
| -27°3544 | M0 Iab | 239.2 | -10.3 | 3.43 | 3.59 | 1.72 | 1.32 | 2.32 | 2.93 | - | 3.92 | - | 3-2 | |
| -26°11359 | M1 Iab+B | 351.9 | +15.1 | 0.96 | 3.12 | 1.82 | 1.57 | 2.92 | 3.51 | 4.43 | 4.66 | 5.00 | 2-2 | * |



© American Astronomical Society • Provided by the NASA Astrophysics Data System

1970ApJ...162..217L



NOTES TO TABLE 1

(Notes refer to entries marked with an asterisk.)

−27°12032: Variable (KW Sgr), Mean Epoch = J.D. 2440008.
−22°4575: Variable (VX Sgr), Mean Epoch = J.D. 2440120.
Case 48: Variable (FR Sct), Mean Epoch = J.D. 2440120.
−12°5055: Variable (UY Sct), Mean Epoch = J.D. 2440005.
+00°4064: Variable (UW Aql), Mean Epoch = J.D. 2440008.
Case 55: Variable (V492 Aql), Mean Epoch = J.D. 2440120.
+10°3721: Variable, Mean Epoch = J.D. 2439986.
+22°3840: Variable, Mean Epoch = J.D. 2440118.
+25°4097: Variable, Mean Epoch = J.D. 2439960.
+29°3730: Variable, Mean Epoch = J.D. 2440001.
Case 61: Variable (V717 Cyg), Mean Epoch = J.D. 2440125.
+36°4025: Variable (BI Cyg), Mean Epoch = J.D. 2439836.
Case 68: Variable (V441 Cyg), Mean Epoch = J.D. 2440111.
+37°3903: Variable (BC Cyg), Mean Epoch = J.D. 2439834.
Case 66: Variable (KY Cyg), Mean Epoch = J.D. 2440120.
+39°4208: Variable (RW Cyg), Mean Epoch = J.D. 2440120.
+45°3349: Variable (AZ Cyg), Mean Epoch = J.D. 2439830.
+58°2316: Variable ($\mu$ Cep), Mean Epoch = J.D. 2440019.
+61°2134: Variable (SW Cep), Mean Epoch = J.D. 2439828.
+55°2737: Variable (RW Cep), Mean Epoch = J.D. 2439773.
+58°2396: Variable (AZ Cep), Mean Epoch = J.D. 2440122.
+56°2793: Variable (ST Cep), Mean Epoch = J.D. 2439772.
+62°2007: Variable (VV Cep), Mean Epoch = J.D. 2439829.
+54°2863: Variable (U Lac), Mean Epoch = J.D. 2439773.
+57°2750: Variable (V358 Cas), Mean Epoch = J.D. 2440118.
+60°2613: Variable (PZ Cas), Mean Epoch = J.D. 2439772.
+60°2634: Variable (TZ Cas), Mean Epoch = J.D. 2439772.
+61°0008: Variable (KN Cas), Mean Epoch = J.D. 2439834.
+62°0207: Variable (HS Cas), Mean Epoch = J.D. 2439831.
+60°0310: Variable (AZ Cas), Mean Epoch = J.D. 2439775.
+54°0444: Variable (XX Per), Mean Epoch = J.D. 2439831.
+58°0501: Variable (GP Cas), Mean Epoch = J.D. 2439517.
+57°0647: Variable, Mean Epoch = J.D. 2439700.
+59°0594: Variable, Mean Epoch = J.D. 2439761.
Case 33: Variable Mean Epoch = J.D. 2440112.
+54°739: Class III (Humphreys 1969), suspect; $E_{B-V} > 1.0$ mag.
+49°1488: Variable ($\psi'$ Aur), Mean Epoch = J.D. 2439520.
+38°1162: Variable, Mean Epoch = J.D. 2440121.
+46°1271: Variable (Y Lyn), Mean Epoch = J.D. 2439522.
+18°0875: Variable (CE Tau), Mean Epoch = J.D. 2439960.
+23°1243: Variable (WY Gem), Mean Epoch = J.D. 2439833.
+22°1220: Variable (BU Gem), Mean Epoch = J.D. 2439518.
+21°1146: Variable (TV Gem), Mean Epoch = J.D. 2439520.
+07°1055: Variable ($\alpha$ Ori), Mean Epoch = J.D. 2440120.
−26°11359: Variable ($\alpha$ Sco), Mean Epoch = J.D. 2440010.

Table 2 contains the observations of a limited number of brighter late-type stars—mostly K- and late M-type giants. These stars are included here so that a good comparison of the intrinsic colors of giants and supergiants can be made. Some of the observations in Table 2 are from the photometry files of Dr. Harold Johnson and were incorporated with those made in this study in order to present the best possible colors and magnitudes. Almost all the $V - H$ color indices, however, were determined by the author and are presented here for the first time. Table 2 is arranged in the same manner as Table 1; however, the stars are identified by their BS numbers (Hoffleit 1964), and the galactic coordinates are omitted.

© American Astronomical Society • Provided by the NASA Astrophysics Data System

TABLE 2

Brighter Late-type Stars

| | Star | Spectrum | V | U-V | B-V | V-R | V-I | V-J | V-H | V-K | V-L | N | Note |
|---|---|---|---|---|---|---|---|---|---|---|---|---|---|
| BS | 45 | M2$^+$ IIIab | 4.80 | 3.50 | 1.57 | 1.34 | 2.47 | 3.17 | 3.95 | 4.17 | 4.34 | 9-9 | @ |
| | 103 | M4 IIIb | 5.06 | 3.47 | 1.65 | 1.74 | 3.28 | 4.01 | 4.94 | 5.19 | 5.40 | 5-4 | * |
| | 258 | sgK1 | 5.45 | 1.92 | 1.01 | 0.77 | 1.27 | 1.69 | 2.22 | 2.30 | 2.35 | 4-2 | |
| | 337 | M0$^+$ IIIab | 2.05 | 3.53 | 1.57 | 1.24 | 2.24 | 2.86 | 3.68 | 3.88 | 4.14 | 4-5 | @ |
| | 495 | sgK2 | 6.32 | 1.99 | 1.04 | 0.73 | 1.21 | 1.68 | 2.15 | 2.26 | 2.31 | 4-3 | |
| | 617 | K2 III | 2.00 | 2.28 | 1.15 | 0.84 | 1.46 | 1.90 | 2.49 | 2.63 | 2.74 | 9-9 | @ |
| | 834 | K3 Ib + B9 V | 3.79 | 3.59 | 1.69 | 1.23 | 2.12 | 2.74 | 3.51 | 3.70 | 3.89 | 2-7 | @ |
| | 867 | M6$^-$ IIIab | 5.93 | 2.63 | 1.51 | 2.42 | 4.59 | 5.69 | 6.63 | 6.98 | 7.17 | 3-3 | * |
| | 911 | M2 IIIab | 2.53 | 3.57 | 1.64 | 1.35 | 2.51 | 3.09 | 3.95 | 4.17 | 4.29 | 6-4 | @ |
| | 1009 | M0$^+$IIa | 5.19 | 4.34 | 2.05 | 1.60 | 2.83 | 3.63 | 4.53 | 4.78 | 4.95 | 2-3 | |
| | 1105 | S5$_3$ | 5.11 | 3.45 | 1.63 | 1.64 | 3.03 | 3.80 | 4.70 | 4.94 | 5.12 | 4-3 | |
| | 1112 | K4 Ib | 5.75 | 3.56 | 1.74 | 1.32 | 2.34 | 3.01 | 3.86 | 4.07 | 4.28 | 3-3 | |
| | 1231 | M0 III | 2.94 | 3.58 | 1.60 | 1.26 | 2.26 | 2.81 | 3.63 | 3.82 | 3.91 | 3-6 | @ |
| | 1286 | cK5 | 5.74 | 2.91 | 1.46 | 1.05 | 1.84 | 2.38 | 3.11 | 3.25 | 3.34 | 3-3 | |
| | 1457 | K5$^+$ IIIab | 0.86 | 3.46 | 1.54 | 1.23 | 2.17 | 2.70 | 3.45 | 3.67 | 3.86 | 9-9 | *@ |
| | 2018 | M3 III | 6.28 | 3.79 | 1.73 | 1.62 | 3.03 | 3.88 | 4.79 | 5.02 | 5.20 | 3-3 | |
| | 2286 | M3$^+$ IIIa | 2.87 | 3.50 | 1.64 | 1.57 | 2.95 | 3.60 | 4.46 | 4.72 | 4.90 | 3-5 | @ |
| | 2615 | cK4 | 5.68 | 3.39 | 1.63 | 1.26 | 2.09 | 2.76 | 3.54 | 3.74 | 3.90 | 1-3 | |
| | 2990 | K0 III | 1.14 | 1.86 | 1.00 | 0.75 | 1.25 | 1.63 | 2.11 | 2.25 | 2.36 | 9-9 | @ |
| | 3249 | K4 III | 3.53 | 3.25 | 1.48 | 1.12 | 1.90 | 2.48 | 3.25 | 3.41 | 3.54 | 9-9 | @ |
| | 3639 | M6 III: S | 5.95 | 2.70 | 1.67 | 2.89 | 5.22 | 6.32 | 7.29 | 7.60 | 7.95 | 3-4 | * |
| | 4057-8 | K0 III-G7 III | 1.98 | 2.15 | 1.15 | 0.85 | 1.47 | 1.89 | 2.53 | 2.65 | 2.78 | 6-9 | @ |
| | 4267 | M5$^+$ IIIa | 5.78 | 2.67 | 1.46 | 2.25 | 4.34 | 5.31 | 6.22 | 6.50 | 6.77 | 2-4 | * |
| | 4517 | M1 IIIab | 4.04 | 3.28 | 1.50 | 1.26 | 2.27 | 2.92 | 3.78 | 3.95 | 4.10 | 5-9 | @ |
| | 4910 | M3$^+$ IIIa | 3.38 | 3.38 | 1.59 | 1.53 | 2.86 | 3.51 | 4.36 | 4.59 | 4.78 | 6-7 | @ |
| | 5299 | M4$^+$ IIIa | 5.28 | 3.24 | 1.58 | 1.85 | 3.51 | 4.42 | 5.41 | 5.57 | 5.81 | 3-9 | @ |
| | 5340 | K2 IIIp | -0.05 | 2.51 | 1.23 | 0.97 | 1.62 | 2.03 | 2.76 | 2.90 | 3.07 | 9-9 | @ |
| | 5589 | M4.5 III | 4.59 | 3.18 | 1.59 | 1.86 | 3.57 | 4.34 | 5.26 | 5.52 | 5.71 | 3-6 | *@ |
| | 5854 | K2 III | 2.64 | 2.42 | 1.17 | 0.81 | 1.37 | 1.88 | 2.46 | 2.57 | 2.64 | 9-9 | @ |
| | 5932 | M3$^+$ IIIa | 5.38 | 3.59 | 1.64 | 1.48 | 2.73 | 3.49 | 4.36 | 4.58 | 4.78 | 9-8 | @ |
| | 5947 | K3 III | 4.15 | 2.51 | 1.23 | 0.89 | 1.51 | 2.06 | 2.73 | 2.85 | 3.00 | 9-9 | @ |
| | 6146 | M6 IIIab | 5.05 | 2.68 | 1.53 | 2.54 | 4.77 | 5.75 | 6.71 | 7.02 | 7.27 | 5-6 | *@ |
| | 6406 | M5 II+G5 III | 3.06 | 2.45 | 1.45 | 2.14 | 4.27 | 5.19 | 6.15 | 6.46 | 6.73 | 6-4 | *@ |
| | 6497 | G2 Ib | 6.04 | 0.87 | 0.60 | 0.61 | 1.04 | 1.48 | 1.98 | 2.07 | 2.19 | 3-3 | |
| | 6603 | K2 III | 2.77 | 2.41 | 1.17 | 0.82 | 1.39 | 1.86 | 2.45 | 2.55 | 2.65 | 9-9 | @ |
| | 6702 | M5$^+$ IIab | 6.32 | 3.13 | 1.61 | 2.17 | 4.07 | 5.01 | 5.94 | 6.21 | 6.47 | 2-2 | * |
| | 7009 | M5 IIab | 6.05 | 3.04 | 1.62 | 2.21 | 4.17 | 5.03 | 6.00 | 6.30 | 6.57 | 3-3 | * |
| | 7892 | K3 Ib | 5.63 | 3.19 | 1.53 | 1.02 | 1.77 | 2.37 | 3.11 | 3.26 | 3.43 | 2-2 | |
| | 7949 | K0 III | 2.46 | 1.90 | 1.03 | 0.73 | 1.27 | 1.69 | 2.26 | 2.35 | 2.46 | 8-9 | @ |
| | 8062 | M4 IIIa: S | 6.23 | 3.50 | 1.67 | 1.77 | 3.33 | 4.16 | 5.04 | 5.31 | 5.53 | 3-4 | |
| | 8775 | M3 IIIa | 2.50 | 3.50 | 1.65 | 1.57 | 2.88 | 3.54 | 4.45 | 4.70 | 4.93 | 2-3 | * |
| | 8989 | M2 III | 6.58 | 4.00 | 1.88 | 1.67 | 3.00 | 3.83 | 4.79 | 5.08 | 5.30 | 3-3 | |

© American Astronomical Society • Provided by the NASA Astrophysics Data System

1970ApJ...162..217L



NOTES TO TABLE 2

BS 0103: Variable (TV Psc), Mean Epoch = J.D. 2440125.
BS 0867: Variable (RZ Ari), Mean Epoch = J.D. 2441025.
BS 1457: Variable ($\alpha$ Tau), possibly variable.
BS 3639: Variable (RS Cnc), Mean Epoch = J.D. 2439965.
BS 4267: Variable (VY Leo), Mean Epoch = J.D. 2439921.
BS 5589: Variable (RR UMi), Mean Epoch = J.D. 2438450.
BS 6146: Variable (g Her), Mean Epoch = J.D. 2439957.
BS 6406: Variable ($\alpha$ Her), Mean Epoch = J.D. 2440010.
BS 6702: Variable (OP Her), Mean Epoch = J.D. 2439960.
BS 7009: Variable (XY Lyr), Mean Epoch = J.D. 2439975.
BS 8775: Variable ($\beta$ Peg), Mean Epoch = J.D. 2440125.

@ Several observations taken from the photometry files of Dr. H L Johnson are included with those made in this study. The author gratefully acknowledges the permission given by Dr. Johnson to use these data, many of which have not been published elsewhere

## III. INTRINSIC PROPERTIES

### *a) Color Indices*

Intrinsic (unreddened) color indices have been determined for M-type giants and supergiants and are given as a function of MK spectral class in Table 3A. The analysis for the giants, for which the pertinent data of Johnson *et al.* (1966) were included as well as those of Table 2, is straightforward since most of these stars are less than 100 pc distant and are unreddened (Kron 1958; Johnson 1966; Fitzgerald 1967). The quoted colors, therefore, are simply the mean values for each spectral class. The $U - I$ and $V - I$ indices of Table 3A are in reasonable agreement with those found by Deutsch, Wilson, and Keenan (1969)—within 0.5 spectral subclass—and the $UBV$ colors are in similar accord with those found by Blanco (1965) and Fitzgerald (1967). The infrared colors of the latest M giants are slightly redder than those of Johnson (1966).

The intrinsic colors of the M supergiants are more difficult to determine as nearly all the stars in Table 1 are located within 5° of the galactic plane and are significantly reddened. However, two-color diagrams ($V - R$ versus $B - V$, $V - I$ versus $B - V$, etc.) similar to the one shown in Figure 1 provide a means of correcting for the reddening. In Figure 1, which includes only stars having reliable spectral types, stars of the same spectral type but with varying amounts of reddening define a linear relation for which the slope is simply the excess ratio, $E_{V-I}/E_{B-V}$. Extrapolations of these loci to the appropriate values of $(B - V)_0$ yield the other unreddened indices. The $(B - V)_0$ dependence on spectral type given in Table 3B followed from an analysis of other results (Blanco 1954; Sharpless 1958; Feinstein 1959; Starikova 1960; Wildey 1964; Johnson 1966, 1967; Fitzgerald 1967) as well as the data for the least reddened supergiants of Table 1. The star $\sigma$ CMa (M0 Iab, $B - V = 1.72$ mag), for example, is near the southern cluster Collinder 121, and may be a member (Feinstein 1967); in this case $(B - V)_0 \cong 1.70$ mag since the mean cluster reddening is $E_{B-V} \leq 0.03$ mag. The $(B - V)_0$ colors given in Table 3B are slightly redder than those of Johnson (1966) but not as red as those quoted by Starikova (1960) or Allen (1964). The other color indices, as determined from the two-color plots, are redder than those of the giants and also show a larger dispersion. This lack of homogeneity is not surprising and undoubtedly results from several factors: poorly determined spectral types, extinction-law variations, spectral-type changes in the case of known variables, circumstellar phenomena, etc. The $V - R$ and $V - I$ colors, however, show less dispersion; and, as shown conclusively for the M giants (Deutsch *et al.* 1969), $V - I$ is a useful indicator of spectral class. The situation for the supergiants is complicated by interstellar extinction, yet the spectral definition seen in Figure 1 is sufficient for meaningful spectral class estimates. Such estimates were used to augment the spectroscopic data for the stars of Table 1. A luminosity distinction is indicated in the $V - H$ and $V - L$ intrinsic colors of the supergiants; additional discussion of this effect will be given in § III*d*.

When a nominal reddening correction is applied, the colors of most of the M super-

© American Astronomical Society • Provided by the NASA Astrophysics Data System

1970ApJ...162..217L

TABLE 3

EFFECTIVE TEMPERATURES, BOLOMETRIC CORRECTIONS, AND INTRINSIC COLORS OF M-TYPE STARS

| Spectrum | $T_{eff}$ | B.C. | $U-V$ | $B-V$ | $V-R$ | $V-I$ | $V-J$ | $V-H$ | $V-K$ | $V-L$ |
|---|---|---|---|---|---|---|---|---|---|---|
| | | | | | A. Giants | | | | | |
| M0 III... | 3700 | −1.14 | 3.42 | 1.56 | 1.24 | 2.14 | 2.77 | 3.57 | 3.74 | 3.89 |
| M1 III... | 3650 | −1.24 | 3.48 | 1.58 | 1.29 | 2.24 | 2.89 | 3.72 | 3.90 | 4.06 |
| M2 III... | 3550 | −1.45 | 3.52 | 1.61 | 1.37 | 2.45 | 3.12 | 3.96 | 4.16 | 4.33 |
| M3 III... | 3350 | −1.81 | 3.46 | 1.62 | 1.52 | 2.82 | 3.53 | 4.39 | 4.63 | 4.81 |
| M4 III... | 3150 | −2.42 | 3.29 | 1.62 | 1.78 | 3.38 | 4.19 | 5.07 | 5.34 | 5.54 |
| M5 III... | 2950 | −3.15 | 3.04 | 1.59 | 2.13 | 4.06 | 4.96 | 5.90 | 6.20 | 6.44 |
| M6 III... | 2750 | −4.10 | 2.70 | 1.58 | 2.70 | 4.90 | 5.90 | 6.87 | 7.20 | 7.50 |
| | | | | | B. Supergiants | | | | | |
| M0 I.... | 3600 | −1.18 | 3.60 | 1.69 | 1.21 | 2.19 | 2.83 | 3.63* | 3.82 | 4.05‡ |
| M1 I.... | 3550 | −1.30 | 3.62 | 1.70 | 1.28 | 2.32 | 2.98 | 3.79* | 3.98 | 4.21‡ |
| M2 I.... | 3450 | −1.55 | 3.64 | 1.71 | 1.41 | 2.56 | 3.25 | 4.08† | 4.31 | 4.55§ |
| M3 I.... | 3200 | −2.04 | 3.62 | 1.73 | 1.61 | 2.98 | 3.75 | 4.65† | 4.91 | 5.18§ |
| M4 I.... | 2950 | −2.55 | 3.60 | 1.77 | 1.85 | 3.44 | 4.32 | 5.26† | 5.52 | 5.88§ |
| M5 I.... | 2800 | −3.3 | 3.4 | 1.8 | 2.2 | 4.0 | 5.0 | 6.0† | 6.3 | 6.7§ |

* For Ia, subtract 0.05 mag.
† For Ia, subtract 0.10 mag.
‡ For Ia, add 0.05 mag
§ For Ia, add 0.10 mag.

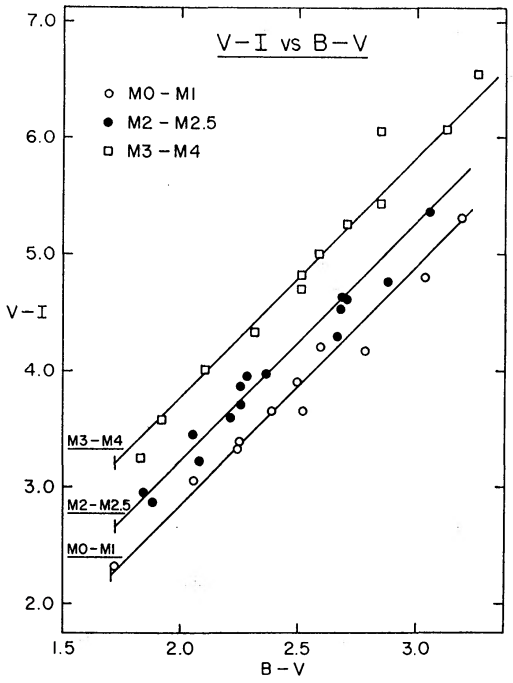


FIG. 1.—$V - I$ versus $B - V$ for M supergiants. Colors of stars with the most reliable spectral types are plotted. The linear relation for each group, M0–M1, M2–M2.5, and M3–M4, is caused by reddening. The slope of the lines is $E_{V-I}/E_{B-V}$.

© American Astronomical Society • Provided by the NASA Astrophysics Data System

1970ApJ...162..217L



giants in Table 1 are commensurate with the intrinsic values quoted for their spectral types (Table 3B). In the Perseus Double Cluster, however, the situation is more complicated. While the present program includes no stars in h and $\chi$ Per, Johnson and Mendoza V. (1966), using the same photometric system employed here, observed seventeen M supergiants in the Double Cluster; twelve of these stars have infrared colors that are *distinctly bluer* than those of comparably reddened stars ($E_{B-V} = 0.6$ mag) in Table 1. The problem, summarized in the data given in Table 4, could be due to an abnormal extinction law for the blue (Group II) M supergiants. However, the Group I stars and Group II stars are not spatially segregated; moreover, localized anomalies of the type

TABLE 4

M SUPERGIANTS IN h AND $\chi$ PERSEI
(Johnson and Mendoza V. 1966)

| Group | Mean $E_{B-V}$ (mag) | Mean $E_{V-L}/E_{B-V}$ |
|---|---|---|
| I: | | |
| +58°373 (M0), +55°597 (M3.5 Iab), +57°552 (M4e Ia), +56°595 (M0.5 Iab) | 0.56 | 3.5±0.3* |
| II: | | |
| +55°529 (M2 Ib), +57°524 (M0.5), +56°512 (M3.5 Ib), +58°439 (M2 Iab), +58°445 (M1), +56°547 (M2.5 Iab), +56°551 (M1 Iab), +57°550 (M1 Ib), +56°583 (M4.5 Iab), +56°597 (M0 Iab), +56°609 (M3 Iab), +56°673 (M2.5 Iab) | 0.59 | 2.7±0.2* |
| +60°478 (M2 Iab) | 1.45: | 4.4: |
| All seventeen stars | 0.65 | 3.0±0.4* |
| Other M supergiants in I Per area ($l^{II}$=100°–150°) | 0.85 | 3.6±0.3* |

* Mean error.

required to account for the bluer stars (low color excess ratios, $R = A_V/E_{B-V} < 3.0$) are rare (Johnson 1968). The extinction law exhibited by the M supergiants in Group I is very similar to that found for the other stars of Table 1 (see § IV). Therefore, the Group II stars in Table 4, as well as $\alpha$ Ori, the only other abnormally blue M supergiant in Table 1, may represent a real subgrouping among these stars. The theoretical results of Stothers and Chin (1968) predict two evolutionary phases for M supergiants, the first during core helium burning, the second (after the blue-supergiant phase) during core carbon burning, neon burning, etc. Because of neutrino losses, the second phase is very brief; consequently, most observable M supergiants should be in the helium-burning stage. If the Group II stars in the Perseus Double Cluster do represent a real minority group of M supergiants, then they could be the second-phase (carbon burning) stars of Stothers and Chin (1968). Yet, why are these M supergiants found only in h and $\chi$ Per (which have an abnormally high number of M supergiants), where they appear to constitute a majority? Clearly, the available observations cannot be pushed any further; since variations in chemical composition could also be important, high-dispersion spectra of

© American Astronomical Society • Provided by the NASA Astrophysics Data System

1970ApJ...162..217L



the stars in Table 4 could be conclusive in resolving this question. Since the evidence is not decisive regarding these "blue" M supergiants, and since they are not seen in other observable parts of the Galaxy, we shall not refer to them in subsequent parts of this paper; the derived colors, bolometric corrections, etc., will apply only to the "normal" M supergiants found in Table 1.

### *b) Bolometric Corrections and Effective Temperatures*

The intrinsic colors of Table 3, together with the absolute flux calibration of the photometric system (Johnson 1966), were used to obtain the spectral energy distribution (from 0.36 to 3.4 $\mu$) commensurate with each spectral type. Bolometric corrections (B.C.) were then computed from integrations of the energy distributions and the use of Johnson's (1964) colors for the Sun—B.C. of Sun normalized to zero. Because of the low temperatures of the late-type stars considered here, no corrections for unobserved ultraviolet radiation were needed; estimates of the flux beyond 3.4 $\mu$ were made from the 5- and 10.2-$\mu$ observations of Wildey and Murray (1964) and Low and Johnson (1964). Even when the large 10.2-$\mu$ fluxes for $\mu$ Cep and $\alpha$ Ori found in these studies is allowed for, the long-wavelength contribution is small. The errors of the bolometric corrections of the giants are due primarily to the uncertainty in the calibration, which may exceed 10 percent. For the supergiants, errors in the intrinsic colors are also significant. Estimates of the maximum probable errors (one observation) of the bolometric corrections given in Table 3 are: giants, 15 percent; supergiants, 20 percent.

Calculation of the effective temperatures requires knowledge of both the total observed flux and the stellar radius. These data, particularly the latter, are in very short supply; therefore, other methods of estimating $T_{\rm eff}$ are often employed. The values of $T_{\rm eff}$ presented here have resulted from an analysis similar to that used by Johnson (1964, 1966). Certain color indices for the limited number of stars having diameter and total-flux measurements are plotted against their computed $T_{\rm eff}$. Interpolations of this relationship then give values of $T_{\rm eff}$ for stars of other colors. The values in Table 3 represent the means of three determinations: (*a*) the calibration of $(I + R) - (J + K)$ versus $T_{\rm eff}$; (*b*) the calibration of $I - L$ versus $T_{\rm eff}$, and (*c*) blackbody temperature in the 1- to 3-$\mu$ region. In general, the three estimates are reasonably accordant; however, the differences for the M5 and M6 giants are near 300° K (the blackbody values are the highest), and therefore the quoted values for these stars have the greatest uncertainty. The three values of $T_{\rm eff}$ for the supergiants are in better agreement as the spread is usually less than 100° K. No distinction is made for Ia, Iab, and Ib supergiants; owing to their larger $V - L$ indices the Ia stars would have slightly lower $T_{\rm eff}$, but the difference would be less than 50° K. Because of the formidable difficulties in constructing realistic stellar atmospheres for M supergiants, a comparison of the emitted flux and $T_{\rm eff}$ from theoretical calculations with those values found here is not possible. The effective temperatures for the giants are higher than those of the supergiants—a result compatible with the provisional values given by Keenan (1963).

### *c) Absolute Magnitudes*

Because of their low spatial density and affinity for variability, the absolute magnitudes of M supergiants are poorly known. Table 5 gives the results from several sources; the preliminary semitheoretical results (unpublished and subject to revision) of Stothers and Leung (1970), which follow from an application of pulsational theory to well-observed variable M supergiants, are presented here with the authors' permission. The observations in Table 1 yield little additional information regarding supergiant absolute magnitudes, except with regard to magnitude differences, $\Delta M_v$(Iab − Ia), $\Delta M_v$(Ib − Iab). The values of $\Delta M_v$ in Table 5 result from the mean visual magnitudes (corrected for extinction) of Ib, Iab, and Ia stars and the assumption that their mean group distances are proportional to their mean reddening. $\Delta M_v$(Iab − Ia) agrees well with the results of Stothers and Leung (1970), but their values yield a smaller $\Delta M_v$(Ib −

© American Astronomical Society • Provided by the NASA Astrophysics Data System

1970ApJ...162..217L



Iab). If the highest luminosity class I stars were in dustier regions and more highly reddened, the discrepancy could be accounted for. However, $\mu$ Cep (M2 Ia), $\alpha$ Ori (M2 Iab), and $\sigma$ CMa (M0 Iab) are nearby supergiants of high luminosity which do not exhibit excessive reddening or evidence for heavy localized extinction. Therefore, although the highest-luminosity supergiants are more concentrated in the galactic plane (see § V), it is doubtful that this can account for all of the discordance mentioned above. The values adopted in Table 5 are believed to be reasonable mean values based on all available evidence. The errors, however, may approach 0.5 mag, and clearly the subject of absolute magnitudes of M supergiants deserves more attention.

### *d) Luminosity Effects*

A weak distinction in photometric luminosity among the M supergiants was found in the infrared data, and is indicated in Table 3B. In comparison with the other supergiants, the highest-luminosity (Ia) stars tend to show (*a*) a flux deficiency near 1.6 $\mu$ and (*b*) a flux excess at 3.4 $\mu$. This trend is seen in the $J - H$ versus $K - L$ diagram in Figure 2, where the higher-luminosity stars generally populate the upper region of the figure; and it is also evident in similar plots for other colors ($I - J$ versus $J - H$). The effect is not a strong one since several stars of lower assigned luminosities show the same ten-

TABLE 5

ABSOLUTE MAGNITUDES OF M STARS

| Source | Luminosity Class | | | | |
|---|---|---|---|---|---|
| | III | II | Ib | Iab | Ia |
| Blaauw (1963) | −0.4 | −2.4 | −4.8 | −5.6 | −7.0 |
| Allen (1964) | −0.4 | −2.4 | −4.4 | ... | ... |
| Fitzgerald (1967) | −0.6 | −2.4 | −4.8 | −5.3 | −7.0 |
| Stothers and Leung (1970) | ... | ... | −4.7 | −5.6 | −6.5 |
| $\Delta M_v$(Ib − Iab) = +1.8 mag<br>$\Delta M_v$(Iab − Ia) = +0.7 mag } Reddening: see text. | | | | | |
| Adopted | −0.5 | −2.4 | −4.5 | −5.8 | −6.6 |

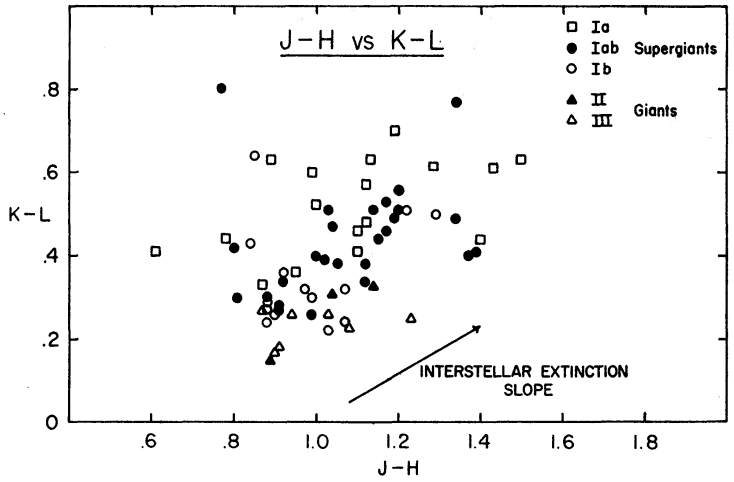


FIG. 2.—$J - H$ versus $K - L$ for M supergiants. Colors of stars with the most reliable luminosity classes are plotted. The trajectory of interstellar reddening, $E_{K-L}/E_{J-H}$, is shown. The highest-luminosity supergiants tend to lie above the other class I stars and giants and suggest a weak luminosity effect.

© American Astronomical Society • Provided by the NASA Astrophysics Data System

1970ApJ...162..217L



dency. Furthermore, the picture is complicated by variability since frequently the highest-luminosity M supergiants also show the largest variations. Therefore, while the effect shown in Figure 2 is most strongly correlated with luminosity, the possibility that it reflects some phase-dependent color changes of these variable stars cannot be eliminated at the present time. Other evidence for long-wavelength ($\lambda > 3.4\ \mu$) excesses for several M Ia stars has been found by Johnson (1967), who suggests that the origin of the radiation is circumstellar. The 1.6-$\mu$ luminosity distinction, however, suggests a different source of continuous infrared opacity for the most luminous M supergiants. Several investigations of late-type stars (Woolf, Schwarzschild, and Rose 1964; McCammon, Münch, and Neugebauer 1967; Bahng 1969) have revealed a continuum maximum near 1.6 $\mu$ which presumably results from the coincidence of a minimum in the $H^-$ bound-free and free-free opacity and the approximate maximum in the Planck distribution. As is shown in Figure 3, the data of this study confirm this result; the intrinsic colors of M

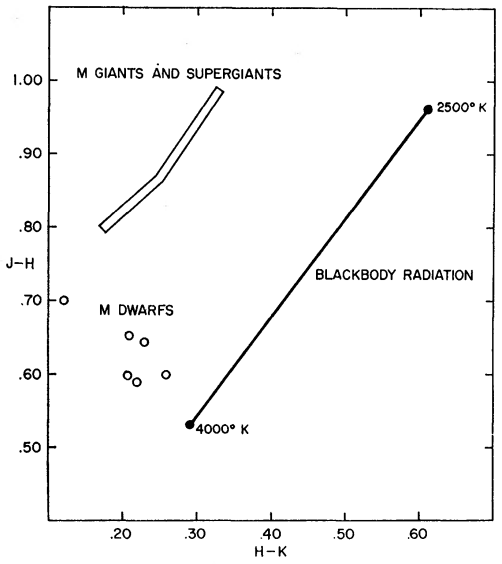


FIG. 3.—$J - H$ versus $H - K$ for M stars. Intrinsic color indices of M supergiants and giants are plotted, as well as the unpublished data for several M dwarfs. The colors of the giants and supergiants deviate significantly from those of blackbodies in the sense of an excess at 1.6 $\mu(H)$; the M dwarfs lie closer to the blackbody relation.

giants and supergiants deviate significantly from those of blackbodies in the sense of a flux excess in the $H(1.6\ \mu)$ band. The excess is not significantly different for giants and supergiants, but observations of several M dwarfs indicate that it is greatly reduced in main-sequence stars. A reduced continuum excess at 1.6 $\mu$ is predicted for dwarfs by the preliminary atmosphere models of Gingerich *et al.* (1966), and results from the increased role of $H_2^-$ in the opacity at higher pressure. The reversed trend among the supergiants, indicated in Figure 2, may suggest that in the tenuous outer atmospheres of Ia stars the opacity becomes dominated by H and $H_2$ Rayleigh scattering (Vardya 1966).

Neither the observational nor the theoretical results justify much additional discussion, except to emphasize some of the problems involved in relating the two. The problem of variability in the M supergiants (and its effect on intrinsic colors) poses many interesting questions, few of which are answered by the observations presented here. Why, for example, are some of these stars variable while others are not? The observations of recognized variables in Table 1 reveal only small changes in $V$ and, in most cases, no variation in the color indices; however, the measurements usually cover only a short time interval. Clearly, the variability of M supergiants is a subject demanding further investi-

© American Astronomical Society • Provided by the NASA Astrophysics Data System

1970ApJ...162..217L



gation. Regarding the theory, stellar-atmosphere calculations for the latest-type stars are plagued by many problems, a very complex equation of state, molecular contributions to the opacity, and the presence of convection, to name a few. In spite of considerable research on the subject, the role of water-vapor opacity in M stars remains a question. The detailed study of Auman (1967) as well as the *Stratoscope II* observations (Woolf *et al.* 1964) of $\alpha$ Ori and $\mu$ Cep indicated that water vapor is present and should be a significant contributor to the opacity in intermediate M supergiants, yet the higher-resolution infrared spectra of Johnson *et al.* (1968) and Thompson *et al.* (1969) showed no trace of the 1.4- and 1.9-$\mu$ $H_2O$ bands in $\alpha$ Ori. Mass loss and the presence of circumstellar material pose additional problems. Weymann (1962) found evidence for circumstellar matter in $\alpha$ Ori with $2 \times 10^{22}$ atoms $cm^{-2}$ in the line of sight; clearly such a cloud could have important effects on the observed "stellar" continuum. Finally, the consequences of varying abundances in M supergiants (which may be important in the Perseus Double Cluster) could be very significant, since they may lead to distinctly different molecular species and opacity sources in the atmospheres of these stars.

## IV. INTERSTELLAR EXTINCTION

### *a) Mean Law of Galactic Extinction*

The foregoing discussion notwithstanding, M supergiants are useful for studies of interstellar extinction since many of them are highly reddened and the uncertainty in their intrinsic colors has a minimal effect. Two-color plots for these stars, similar to the one showing $V - I$ versus $B - V$ in Figure 1, are useful in deriving a mean law of galactic extinction. The linear locus representing each spectral type results from stars having various amounts of differential extinction; the slope of the locus is the color-excess ratio, $E_{V-I}/E_{B-V}$ in the case of Figure 1. Three least-squares solutions, one each for the early, intermediate, and late M supergiants, were carried out for each excess ratio, $E_{V-R}/E_{B-V}$, . . . , $E_{V-L}/E_{B-V}$. The results for the three groups of stars are in good accordance and were used to obtain the mean normalized extinction law shown in Figure 4. The wavelength dependence shown here, which suggests a ratio of total selective absorption of $R = A_V/E_{B-V} \geq 3.5$, should be reliable since no assumptions regarding intrinsic color indices are implicit in the derivation. The value $R = 3.6 \pm 0.3$ (m.e.) results from an extrapolation of the curve to $1/\lambda = 0$. This value is higher than the traditional 3.0; however, the discordance is not large since, because of the wide passbands used for the observations, the same monochromatic extinction law yielding $R = 3.6$ for M stars would give a lower value, approximately 3.3, for hotter O and B stars (Lee 1968). In fact, $R = 3.6$ for M supergiants should be regarded as a lower limit since the methods employed here do not detect extinction that is not wavelength-dependent in the range 0.4–3.4 $\mu$; evidence for such "neutral" extinction has been found by Johnson (1968) and Neckel (1967).

In order to discover regional variations in the extinction wavelength dependence, and also to check the validity of the supergiant intrinsic color indices, the color excesses (observed color minus intrinsic color) of the individual reddened supergiants were computed. Excluded from this analysis are stars with blue companions, stars of low reddening ($E_{B-V} < 0.25$ mag), and stars found to be giants. Regional extinction laws were determined from the excess ratios of stars in 25° intervals of galactic longitude extending from $l^{II} = 0°$ to $l^{II} = 200°$. The mean values of the excess ratios of fifty-three supergiants, weighted by $E_{B-V}$, are given with the standard deviations in Table 6. Also included here are the values resulting from the slopes in the two-color plots. The ratios from the excesses of the individual stars are slightly larger than those obtained from the two-color loci, but the differences are smaller than the mean errors. Therefore, the intrinsic supergiant color indices (Table 3B) are not seriously in error. Determinations of the regional extinction law are hindered by the lack of observations in all areas; the available data, however, reveal no statistically significant deviations from the mean law given in Figure

© American Astronomical Society • Provided by the NASA Astrophysics Data System

1970ApJ...162..217L



4. The errors are such that variations from 3.3 to 3.8 in the value of $R$ obtained from extrapolation of M-supergiant extinction laws to $1/\lambda = 0$ cannot be ruled out; however, these variations as well as the work of Lynds (1967) do not confirm the distinct galactic-longitude dependence of $R$ found by Johnson (1968). Nor is there any evidence in the supergiant observations for "neutral" extinction. Clearly, the extreme extinction laws found in some regions at wavelengths $\lambda \leq 3.4\ \mu$ (Johnson and Borgman 1963; Johnson 1968; Lee 1968) represent very localized phenomena, nearly all of which are found in young open clusters or rich emission nebulosity. While the present data yield no information concerning the extinction law at longer wavelengths, the fact that none of the moderately reddened M supergiants included in this study shows $E_{V-L}/E_{B-V} > 3.9$ is significant evidence against the existence of extensive areas of highly anomalous interstellar extinction in the Galaxy.

*b) Distribution of Reddening Material*

The coarse distribution of obscuring matter in the galactic plane is readily obtainable from the observations and is shown in the diagrams of Figure 5. The figures show the

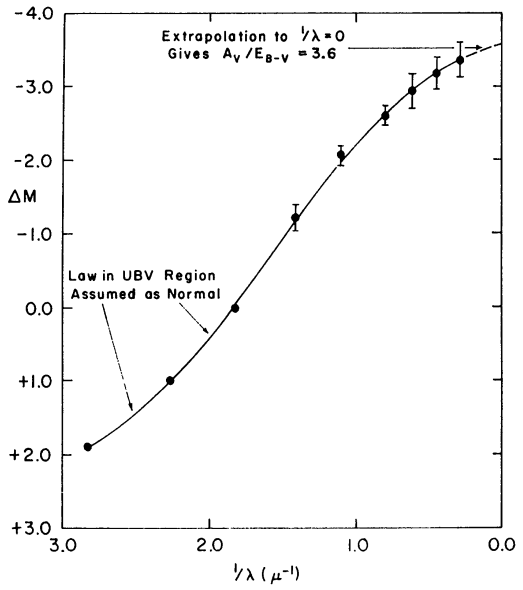


FIG. 4.—Mean law of interstellar extinction. The normalized extinction $\Delta M_V$ ($E_{B-V} = 1.0$ mag) is plotted against $1/\lambda$. The law results from two-color plots (similar to Fig. 1) for distant M supergiants. Error bars represent twice the mean error of one observation. The law in the blue and visual regions is assumed to be "normal"—like van de Hulst's (1949) curve No. 15. Extrapolation to $1/\lambda = 0$ gives $R = 3.6 \pm 0.3$.

TABLE 6

INTERSTELLAR-EXTINCTION LAW FROM M SUPERGIANTS

| | Mean Slope from Two-Color Diagrams | Mean Ratios of Individual Color Excesses |
|---|---|---|
| $E_{V-R}/E_{B-V}$ | 1.23±0.10* | 1.28±0.10* |
| $E_{V-I}/E_{B-V}$ | 2.05±0.07 | 2.16±0.12 |
| $E_{V-J}/E_{B-V}$ | 2.59±0.07 | 2.63±0.09 |
| $E_{V-H}/E_{B-V}$ | 2.92±0.13 | 3.02±0.12 |
| $E_{V-K}/E_{B-V}$ | 3.17±0.13 | 3.22±0.12 |
| $E_{V-L}/E_{B-V}$ | 3.37±0.13 | 3.38±0.10 |

* Mean error.

© American Astronomical Society • Provided by the NASA Astrophysics Data System

1970ApJ...162..217L



mean dependence of $E_{B-V}$ on distance, as determined from the intrinsic colors of Table 3 and the absolute magnitudes of Table 5, for stars in galactic-longitude intervals of 25°. The value of $E_{B-V}$ given near 0.5 kpc results from the observations of nearby supergiants and giants, whereas the value at greater distances obtains from supergiants only. Stars in all longitude zones show large dispersion in both distance and $E_{B-V}$, yet some definite features are seen in Figure 5. The reddening is the highest in the $l^{II}$ = 50°–100° regions, which include the tangent of the local (Orion) spiral arm. In the anticenter direction ($l^{II}$ = 150°–200°) the extinction is the lowest, although the analysis here is hindered by several stars of uncertain luminosity. The data extend to 3.6 kpc in the 100°–125° zone, and the reddening does not increase proportionally with distance. In general, the results

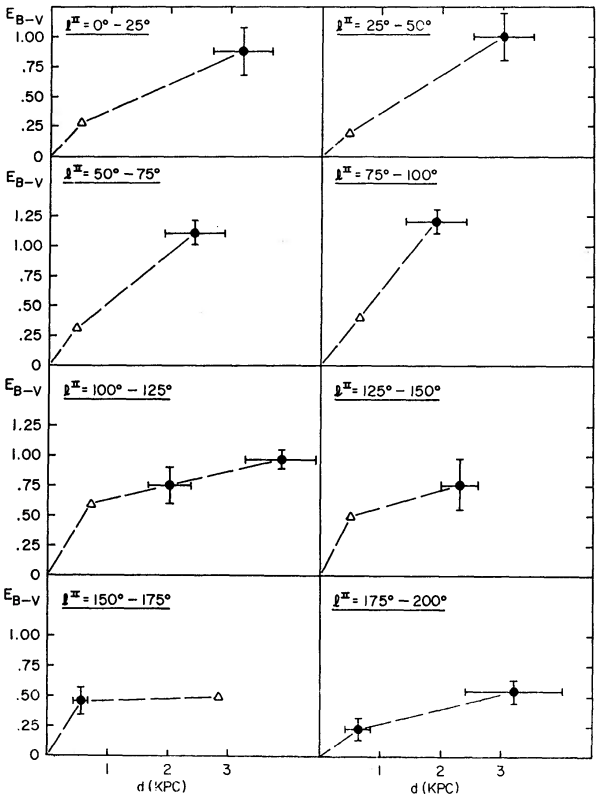


FIG. 5.—Distribution of reddening. Mean value of $E_{B-V}$ and distance are plotted for 25° intervals along the galactic plane. Mean errors are shown for those points determined by the observations of five or more stars. The reddening gradient is highest in the tangent direction of the local spiral arm ($l^{II}$ = 50°–100°) and lowest toward the anticenter.

shown in Figure 5 are compatible with those expected from recognized spiral features (Sharpless 1965) and agree well with the higher-resolution results of Fitzgerald (1967).

### *c) Luminosity Estimates from Reddening*

In one respect the reddening of stars in the galactic plane is useful since it allows one to estimate the luminosity (either class I or class III) if spectroscopic luminosity evidence is lacking. That is, for an M star in the galactic plane, often either class I or class III can be eliminated if the implied reddening per kiloparsec is unreasonable—e.g., an assumed giant ($M_V$ = 0.5 mag) whose distance is 150 pc and whose reddening is $E_{B-V}$ = 1.0 mag. Such estimates, with frequent reference to detailed studies of obscuring matter in the Galaxy (Neckel 1966; Fitzgerald 1967), were required for some stars included in this

© American Astronomical Society • Provided by the NASA Astrophysics Data System

1970ApJ...162..217L



study; luminosity assignments based on this criterion are given in parentheses in Table 1 and, of course, are of lower weight.

## V. SPATIAL DISTRIBUTION OF M SUPERGIANTS

The distribution of M supergiants and probable M supergiants in galactic coordinates is shown in Figure 6, *a;* those stars observed by Humphreys (1969) but not included in Table 1 are also shown, as well as the position of the Perseus Double Cluster. Figure 6, *c*, gives the schematic density distribution of O- and B-type stars according to the data of Hiltner (1956). The analogous plot of M supergiants, if Hiltner's (1956) longitude intervals are adopted, is given in Figure 6, *b*, and shows a striking resemblance to that of

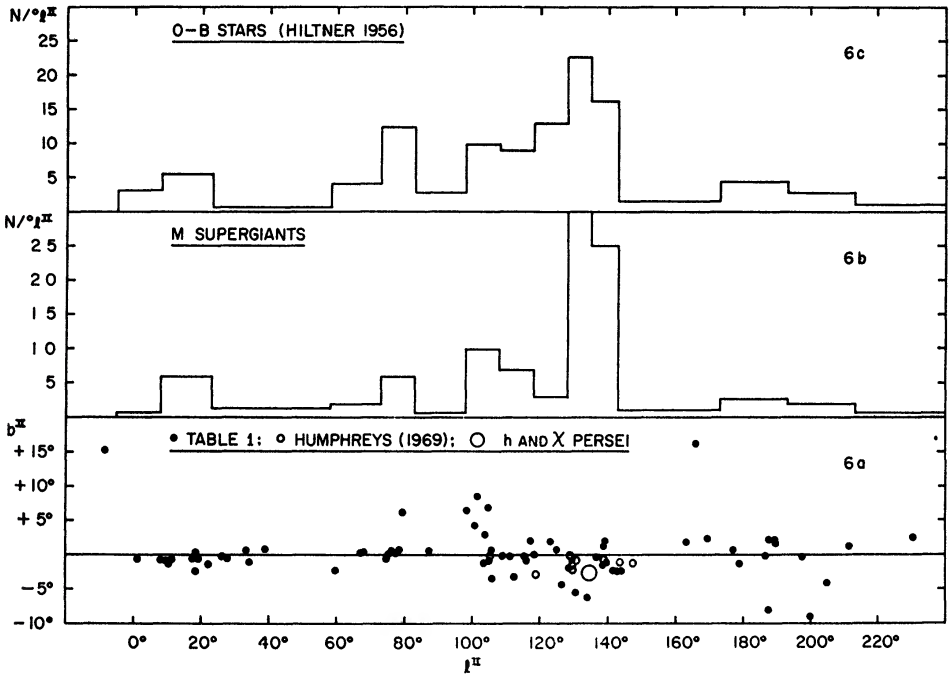


FIG. 6.—Longitude distribution of M supergiants. (*a*) Galactic coordinates of M supergiants and probable M supergiants are plotted. Several additional stars observed by Humphreys (1969) are also shown (*circles*), as well as the Perseus Double Cluster. (*b*) Analogous distribution for M supergiants, if Hiltner's (1956) longitude intervals are used. It is seen to be very similar to that of the O–B stars. (*c*) Schematic distribution of O–B stars, from the survey of Hiltner (1965).

the O and B stars. The broad density minimum at $l^{II} = 150°$ results in part from high obscuration by nearby dust clouds (Heeschen 1951), as may several other star-deficient regions. Nevertheless, the similarity in Figure 6, *b* and *c*, reflects the youth of M supergiants and their classification as stars of the extreme Population I type. The low spatial density of M supergiants is very evident from the numbers of O and B stars and M supergiants included in Figure 6; the observations are probably of comparable completeness ($V \cong 9$) for both groups of stars, yet the average M supergiant will be more luminous than the average O or B star. Therefore, the number of observed O and B stars and M supergiants give an approximate upper limit to their relative densities—$N_{MSG}/N_{OB} < 108/1259 < 0.1$.

The distances of individual supergiants were determined from their spectroscopic distance moduli. The interstellar-extinction correction for each star was taken as the mean of two values: (1) $3.6 \times E_{B-V}$ and (2) $1.1 \times E_{V-L}$. This mean $A_V$ gives equal weight to (1) the uniform extinction law found in § IV and (2) the individual infrared excesses

© American Astronomical Society • Provided by the NASA Astrophysics Data System

1970ApJ...162..217L



which may reveal minor extinction-law variations; yet it minimizes the effects of anomalous intrinsic colors and spectral-type errors. In nearly all cases the two values of $A_V$ agree very closely, and therefore the extinction correction is well determined. Unfortunately, the uncertainty in the absolute magnitudes is larger and may approach $\pm 0.5$ mag, which causes a 25 percent uncertainty in the computed distances. Since many M supergiants are variable, the errors may be even larger for some stars. The data on spatial distribution for M supergiants are summarized in Table 7 and include: star name; galactic coordinates; visual extinction; absolute magnitude; distance (kiloparsecs), and $Z$ distance (kiloparsecs). The Remarks column shows a colon for stars with uncertain luminosity classes as well as possible association membership based on the data given by Sharpless (1965).

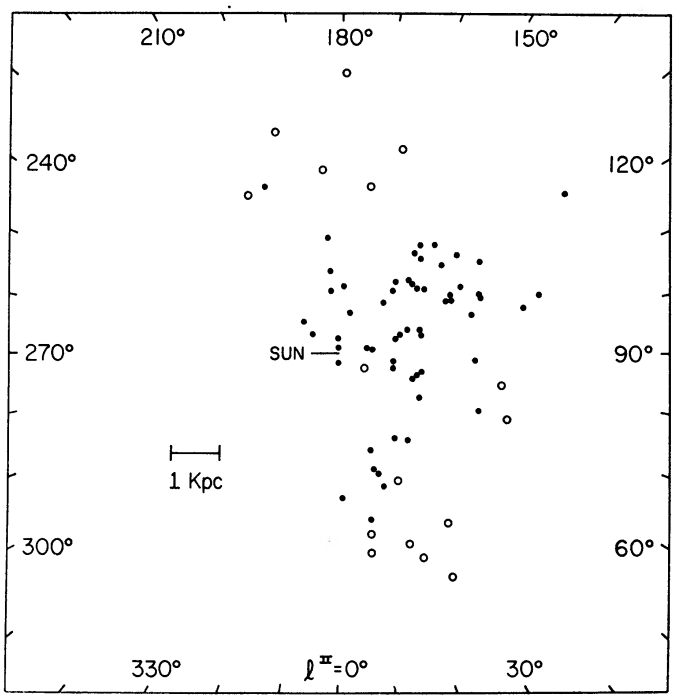


FIG. 7.—Spatial distribution of M supergiants projected on the galactic plane. Distances of individual supergiants from the Sun are shown. *Open circles*, positions of probable supergiants, whose luminosities are more uncertain. Although the scatter is large, some evidence of the familiar spiral features is seen.

The distribution of stars in the galactic plane is shown in Figure 7; only class I stars and probable class I stars (*open circles*) are shown in this diagram. Although the scatter is considerable, the distribution shows some semblance of the spiral structure exhibited by other Population I tracers (Sharpless 1965). From $l^{II} = 0°$ to $l^{II} = 40°$ the inner (Sagittarius) arm is in evidence; the arm is suggested to a distance of 5 kpc, but most of the distant stars are of lower weight (some are less reddened than the stars near 2 kpc) and may be of lower luminosity. The local (Orion) arm is evident near $l^{II} = 75°$ as well as a distinct inter-arm gap at $l^{II} = 105°$. The Perseus arm is represented from $l^{II} = 105°$ to $l^{II} = 143°$, and an inter-arm lane is also suggested. The abrupt termination of the Perseus arm near $l^{II} = 143°$ is also seen in the distribution of open clusters and associations (Sharpless 1965). The stars in the anticenter direction at distances from 0.9 to 1.7 kpc could represent the familiar bifurcation or spur of the local arm (Morgan, Whitford, and Code 1953); the latitude of the two stars near the Sun (+18°875 and $\alpha$ Ori) is distinctly negative whereas that of the more distant (spur) stars is slightly positive. The

© American Astronomical Society • Provided by the NASA Astrophysics Data System

© American Astronomical Society • Provided by the NASA Astrophysics Data System

TABLE 7

Spatial Distribution Data

| Star | $l^{II}$ | $b^{II}$ | $A_V$ | $M_V$ | d (kpc) | Z (kpc) | R |
|---|---|---|---|---|---|---|---|
| -27°12032 | 01.5 | -0.7 | 3.8 | -6.5 | 3.0 | -0.04 | Anon. |
| -22°4575 | 08.3 | -0.9 | | | | | |
| -21°4897 | 09.8 | -1.0 | 2.3 | -5.6 | 4.2 | -0.07 | : |
| -20°5056 | 10.3 | -1.2 | 3.9 | -5.6 | 3.8 | -0.08 | : |
| -19°4907 | 11.6 | -0.7 | 1.2 | -4.5 | 3.5 | -0.04 | III Sgr: |
| -19°5039 | 13.3 | -4.1 | 0.9 | -0.5 | 0.5 | -0.04 | |
| Case 49 | 17.8 | -0.6 | 4.8 | -5.8 | 2.5 | -0.03 | I Ser |
| -14°5105 | 18.3 | -2.4 | 2.0 | -5.8 | 2.1 | -0.09 | I Ser |
| Case 48 | 18.4 | +0.3 | 4.2 | -5.8 | 2.6 | +0.01 | II Ser |
| -12°5055 | 19.1 | -0.4 | 4.0 | -6.2 | 2.9 | -0.02 | I Ser: |
| -10°4738 | 22.4 | -1.5 | 2.1 | -5.6 | 4.2 | -0.11 | : |
| -08°4645 | 23.2 | -0.6 | 2.7 | -5.6 | 4.6 | -0.05 | : |
| -06°4827 | 25.7 | -0.4 | 3.8 | -5.6 | 2.9 | -0.02 | : |
| -05°4743 | 27.6 | -0.6 | 2.2 | -5.6 | 5.2 | -0.05 | : |
| + 0°4030 | 33.5 | +0.5 | 2.9 | -5.6 | 4.2 | +0.04 | : |
| + 0°4064 | 34.0 | -1.2 | 3.1 | -5.8 | 2.1 | -0.04 | |
| Case 55 | 38.6 | +0.7 | 5.3 | -6.5 | 2.3 | +0.03 | |
| +10°3721 | 42.7 | +4.1 | 0.5 | -0.5 | 0.3 | +0.02 | |
| +09°3920 | 43.2 | +3.1 | 0.9 | -0.5 | 0.6 | +0.03 | : |
| +12°3703 | 44.7 | +5.2 | 0.5 | -0.5 | 0.7 | +0.06 | : |
| +22°3840 | 59.7 | -2.5 | 4.5 | -5.6 | 0.6 | -0.03 | : |
| +24°3902 | 61.6 | -0.7 | 4.4 | -6.5 | 1.9 | -0.02 | I Vul |
| +25°4097 | 64.0 | -3.3 | 2.4 | -2.4 | 0.4 | -0.02 | |
| +29°3730 | 65.8 | +2.8 | 0.3 | -0.5 | 0.4 | +0.02 | |
| Case 61 | 67.9 | +0.3 | 3.4 | -5.8 | 3.2 | +0.02 | |
| Case 62 | 67.9 | +0.3 | 3.0 | -5.6 | 3.8 | +0.02 | |
| +35°4077 | 74.2 | -0.6 | 4.4 | -5.8 | 1.7 | -0.02 | II Cyg |
| +35°4135 | 75.0 | -1.9 | 0.8 | -0.5 | 0.6 | -0.02 | : |
| +36°4025 | 75.3 | +0.2 | 4.5 | -5.8 | 1.3 | 0.00 | II Cyg: |
| Case 68 | 75.7 | -1.0 | | | | | |
| +37°3903 | 75.8 | +0.4 | 5.3 | -6.5 | 1.7 | +0.02 | II Cyg |
| Case 66 | 77.0 | +0.2 | 6.3 | -6.5 | 1.8 | +0.01 | III Cyg |
| +39°4208 | 78.6 | +0.7 | 4.0 | -6.2 | 1.1 | +0.01 | II Cyg |
| +43°3477 | 79.1 | +6.3 | 3.0 | -5.6 | 3.5 | +0.37 | : |
| +45°3349 | 87.1 | +0.5 | 3.0 | -6.5 | 2.9 | +0.03 | |
| +58°2249 | 98.2 | +6.3 | 1.2 | -4.5 | 0.7 | +0.08 | I Cep |
| μ Cep | 100.6 | +4.3 | 1.8 | -6.5 | 0.6 | +0.05 | I Cep |
| +61°2134 | 101.5 | +8.5 | 2.1 | -5.2 | 2.5 | +0.37 | |
| +55°2737 | 103.2 | -1.1 | 2.8 | -7.5 | 1.8 | -0.03 | : |
| +58°2396 | 103.7 | +3.0 | 3.5 | -6.5 | 4.0 | +0.21 | |
| +56°2793 | 104.6 | -0.8 | 2.2 | -4.5 | 1.2 | -0.02 | I Cep: |
| +62°2007 | 104.9 | +7.0 | 1.1 | -6.5 | 1.3 | +0.16 | I Cep: |
| +54°2863 | 105.8 | -3.5 | 2.2 | -5.8 | 2.9 | -0.18 | II Cep |
| Case 75 | 105.9 | +0.6 | 5.0 | -6.5 | 4.4 | +0.05 | II Cep |
| +59°2541 | 106.9 | +2.1 | 1.4 | -0.5 | 0.7 | +0.03 | : |
| Case 78 | 107.9 | 0.0 | 4.5 | -4.5 | 1.5 | 0.00 | |
| Case 79 | 109.3 | +1.6 | | | | | |
| Case 81 | 111.2 | -0.1 | 3.3 | -5.8 | 3.2 | -0.01 | II Cep |
| +57°2750 | 112.3 | -3.2 | 3.0 | -6.5 | 3.2 | -0.18 | II Cep |
| +60°2613 | 115.0 | -0.1 | 3.3 | -6.5 | 2.6 | 0.00 | I Cas |
| +60°2634 | 115.9 | -1.0 | 3.0 | -5.8 | 2.5 | -0.04 | I Cas |
| +64°1842 | 115.9 | +3.7 | 2.9 | -2.4 | 0.7 | +0.04 | |
| +63°2073 | 116.8 | +2.1 | 2.6 | -4.5 | 2.6 | +0.10 | I Cas |
| +61° 08 | 118.2 | +0.1 | 1.7 | -4.5 | 2.9 | +0.01 | I Cas |
| Case 23 | 122.8 | +1.9 | 3.9 | -5.8 | 3.5 | +0.12 | III Cas: |
| +62° 207 | 124.8 | +0.8 | 2.5 | -6.5 | 5.8 | +0.08 | |
| +57° 258 | 126.6 | -4.4 | 1.4 | -4.5 | 2.2 | -0.17 | NGC 457 |
| +59° 274 | 128.1 | -1.7 | 1.4 | -4.5 | 2.1 | -0.06 | NGC 581 |
| +60° 310 | 129.0 | -0.9 | 1.2 | -4.5 | 3.2 | -0.05 | : |
| +55° 388 | 130.1 | -5.6 | 1.1 | -4.5 | 2.8 | -0.27 | I Per: |

© American Astronomical Society • Provided by the NASA Astrophysics Data System

TABLE 7 (continued)

| Star | $l^{II}$ | $b^{II}$ | $A_V$ | $M_V$ | d (kpc) | Z (kpc) | R |
|---|---|---|---|---|---|---|---|
| +54° 444 | 133.1 | -6.2 | 1.2 | -4.5 | 2.1 | -0.23 | I Per |
| +58° 501 | 136.3 | -0.5 | 3.6 | -5.8 | 2.1 | -0.02 | I Per |
| +57° 647 | 138.3 | -1.4 | 3.5 | -6.5 | 3.0 | -0.07 | I Per: |
| +59° 580 | 138.3 | +1.1 | 2.3 | -4.5 | 2.6 | +0.05 | |
| +59° 594 | 139.0 | +1.9 | 3.5 | -5.8 | 1.7 | +0.06 | |
| Case 31 | 139.2 | -1.3 | 3.6 | -4.5 | 1.4 | -0.03 | |
| Case 33 | 141.3 | -2.3 | 5.0 | -5.8 | 1.9 | -0.08 | I Per: |
| +54° 651 | 142.5 | -2.4 | 2.8 | -5.8 | 2.8 | -0.12 | I Per: |
| Case 34 | 142.7 | -2.4 | 3.4 | -5.2 | 2.6 | -0.11 | I Per: |
| +55° 778 | 143.2 | -0.2 | 1.8 | -0.5 | 0.5 | 0.00 | : |
| +54° 739 | 148.7 | +2.4 | 3.8 | -0.5 | 0.2 | +0.01 | : |
| +44°1005 | 160.0 | -1.1 | 2.6 | -0.5 | 0.4 | -0.01 | |
| +42°1065 | 162.0 | -1.0 | 0.7 | -0.5 | 1.0 | -0.02 | : |
| +43°1131 | 162.3 | +0.1 | 0.4 | -0.5 | 0.3 | 0.00 | : |
| +43°1183 | 163.1 | +1.8 | 1.8 | -5.6 | 4.4 | +0.14 | : |
| +39°1070 | 164.3 | -3.2 | 1.4 | -0.5 | 0.6 | -0.03 | |
| Case 39 | 164.6 | -2.6 | 1.9 | -0.5 | 0.6 | -0.03 | |
| +49°1488 | 165.4 | +16.2 | 0.9 | -5.8 | 0.9 | +0.25 | |
| +38°1162 | 169.5 | +2.3 | 2.7 | -5.6 | 3.5 | +0.14 | : |
| +46°1271 | 172.3 | +25.2 | | | | | |
| +31°1049 | 176.9 | +0.7 | 1.3 | -5.8 | 1.4 | +0.02 | I Aur |
| +32°1113 | 177.7 | +3.0 | 0.3 | -0.5 | 0.8 | +0.04 | : |
| +32°1109 | 177.9 | +2.7 | 0.4 | -0.5 | 0.2 | +0.01 | |
| +28° 834 | 179.0 | -1.4 | 1.7 | -5.6 | 5.8 | -0.14 | |
| +24°1072 | 185.4 | +1.3 | 1.1 | -0.5 | 0.6 | +0.01 | |
| +25°1131 | 185.5 | +2.7 | 0.0 | -0.5 | 0.4 | +0.02 | : |
| +23°1138 | 186.1 | -0.1 | 3.0 | -5.6 | 3.8 | -0.01 | : |
| +18° 875 | 187.2 | -8.1 | 1.2 | -4.5 | 0.3 | -0.04 | |
| +23°1243 | 187.9 | +2.2 | 1.3 | -5.8 | 2.4 | +0.09 | I Gem |
| +23°1240 | 188.1 | +2.1 | 0.8 | -0.5 | 0.6 | +0.02 | : |
| +22°1220 | 188.2 | +2.2 | 1.7 | -6.5 | 1.7 | +0.07 | I Gem |
| +21°1146 | 189.1 | +1.6 | 1.9 | -5.8 | 1.3 | +0.04 | I Gem |
| +19°1183 | 190.1 | -1.4 | 0.4 | -0.5 | 0.7 | -0.02 | : |
| +13°1110 | 195.8 | -3.5 | 0.8 | -0,5 | 0.5 | -0.03 | |
| +13°1212 | 197.1 | -0.3 | 2.6 | -5.6 | 4.8 | -0.03 | : |
| +07°1055 | 199.8 | -9.0 | 0.5 | -5.8 | 0.1 | -0.01 | I Ori: |
| +10°1085 | 200.1 | -2.4 | 0.1 | -0.5 | 0.7 | -0.03 | : |
| +05°1198 | 204.3 | -4.2 | 0.9 | -5.8 | 3.8 | -0.28 | |
| +02°1451 | 211.4 | +1.1 | 1.9 | -5.6 | 3.8 | +0.07 | : |
| -09°1649 | 221.3 | -5.4 | 0.4 | -2.4 | 2.2 | -0.21 | |
| -14°1971 | 230.6 | +2.5 | 0.7 | -5.8 | 1.0 | +0.04 | NGC 2422 |
| -27°3544 | 239.2 | -10.3 | 0.1 | -5.8 | 0.7 | -0.13 | Coll 121 |
| -26°11359 | 351.9 | +15.1 | 0.9 | -5.8 | 0.2 | +0.04 | II Sco |

1970ApJ...162..217L



stars at distances greater than 3 kpc (in the anticenter direction) are of lower weight but are more highly reddened than those stars nearer the Sun and may suggest structure in the outermost regions of the Galaxy.

Nearly all the well-classified supergiants of Table 7 are in or near recognized O and B associations; the groups of probable supergiants near $l^{II} = 20°$ and at the anticenter could be members of distant early-type aggregates heretofore unidentified. However, the extreme Population I character of M supergiants is best illustrated by their concentration to the galactic plane. Table 8 summarizes the data regarding $|\langle Z\rangle|$ for the M supergiants in Table 1 as well as that for O and B stars. The value of $|\langle Z\rangle|$ from Hiltner's (1956) data on O and B stars is the mean of a sample of 129 stars (~10 percent of survey) distributed throughout the sky. M supergiants, as a group, show only slightly greater dispersion about the galactic plane than do the O and B stars. Moreover, $|\langle Z\rangle|$ is correlated with luminosity among the supergiants, the Ia stars showing the strongest concentration in the plane. This result is comforting, for it gives credence to the basic theories concerning M supergiants. That is, massive O and B stars evolve rapidly into the M-supergiant stage, the time scales being the shortest for the very highest masses and luminosities (Ia). The Ia supergiants have not moved significantly out of the plane

TABLE 8

DISTRIBUTION PERPENDICULAR TO GALACTIC PLANE

| Stars | Number of Stars | $\lvert\langle Z\rangle\rvert$ (pc) |
|---|---|---|
| M supergiants—all class I and (I) | 73 | 78 (±18) |
| M supergiants Ia | 18 | 60 (±15) |
| M supergiants Iab | 24 | 73 (±16) |
| M supergiants Ib | 13 | 96 (±23) |
| O–B5 (Blaauw 1965) | ... | 50 |
| O–B (Hiltner 1956) | 129 (sample) | 66 |

with respect to O and B stars and therefore must have very similar ages; the less massive M supergiants, which are still high-mass stars ($M \simeq 15\ M_\odot$) have longer total lifetimes and, hence, higher $|\langle Z\rangle|$.

This work was supported in part by the Office of Naval Research (NR 046-798), the National Science Foundation (GP 7827X), and the National Aeronautics and Space Administration (NGR-03-002-180). I wish to extend my thanks to Drs. B. Bok, H. L. Johnson, and R. Stothers for their helpful suggestions and comments; to Drs. K. Leung, R. Stothers, and A. Wawrukiewicz for permission to use their unpublished results; and to Drs. R. Jastrow, A. Levine (Goddard Institute for Space Studies), and G. P. Kuiper (Lunar and Planetary Laboratory) for their hospitality. Most of this work was carried out while the author held a NAS-NRC Postdoctoral Research Associateship at the Goddard Institute for Space Studies.

REFERENCES

Allen, C. W. 1964, *Astrophysical Quantities*, 2d ed. (London: Athlone Press), p. 201.
Auman, J., Jr. 1967, *Ap. J. Suppl.*, **14**, 171 (No. 127).
Bahng, J. 1969, *M.N.R.A.S.*, **143**, 73.
Bidelman, W. P. 1951, *Ap. J.*, **113**, 304.
———. 1954, *Ap. J. Suppl.*, **1**, 175.
———. 1957, *Pub. A.S.P.*, **69**, 326.
Bidelman, W. P., and Stephenson, C. B. 1956, *Pub. A.S.P.*, **68**, 152.
Blaauw, A. 1963, *Basic Astronomical Data*, ed. K. Aa. Strand (Chicago: University of Chicago Press), p. 383.
———. 1965, in *Galactic Structure*, ed. A. Blaauw and M. Schmidt (Chicago: University of Chicago Press), p. 435.

© American Astronomical Society • Provided by the NASA Astrophysics Data System

1970ApJ...162..217L



Blanco, V. M. 1954, *A.J.*, **59**, 396.
———. 1965, in *Galactic Structure*, ed. A. Blaauw and M. Schmidt (Chicago: University of Chicago Press), p. 249.
Blanco, V. M., and Nassau, J. J. 1957, *Ap. J.*, **125**, 408.
Cowley, A. P. 1969, *Pub. A.S.P.*, **81**, 297.
Deutsch, A. J., Wilson, O. C., and Keenan, P. C. 1969, *Ap. J.*, **156**, 107.
Feinstein, A. 1959, *Zs. f. Ap.*, **47**, 218.
———. 1967, *Ap. J.*, **149**, 107.
Fitzgerald, M. P. 1967, dissertation, Case Western Reserve University.
Gahm, G. F., and Zappala, R. R. 1969, *Pub. A.S.P.*, **81**, 887.
Gingerich, O., and Kumar, S. S. 1964, *A.J.*, **69**, 139.
Gingerich, O., Latham, D. W., Linsky, J., and Kumar, S. S. 1966, in *Colloquium on Late Type Stars*, ed. M. Hack (Trieste), p. 291.
Hayashi, C., and Cameron, R. C. 1962, *Ap. J.*, **136**, 166.
Hayashi, C., Hōshi, R., and Sugimoto, D. 1962, *Progr. Theoret. Phys. Suppl.*, No. 22.
Heeschen, D. S. 1951, *Ap. J.*, **114**, 132.
Hiltner, W. A. 1956, *Ap. J. Suppl.*, **2**, 389, (No. 24).
Hoffleit, D. 1964, *Catalogue of Bright Stars* (Yale University Observatory).
Hulst, H. C. van de. 1949, *Rech. Astr. Obs. Utrecht*, Vol. **11**, Part 2.
Humphreys, R. 1969, dissertation, University of Michigan.
Johnson, H. L. 1964, *Bol. Obs. Tonantzintla y Tacubaya*, **3**, 305 (No. 25).
Johnson, H. L. 1966, *Ann. Rev. Astr. and Ap.*, **4**, 193.
———. 1967, *Ap. J.*, **149**, 345.
———. 1968, in *Nebulae and Interstellar Matter*, ed. B. M. Middlehurst and L. H. Aller (Chicago: University of Chicago Press), p. 167.
Johnson, H. L., and Borgman, J. 1963, *B.A.N.*, **17**, 115.
Johnson, H. L., and Mendoza V., E. E. 1966, *Ann. d'ap.*, **29**, 525.
Johnson, H. L., Mitchell, R. I., Iriarte, B., and Wiśniewski, W. 1966, *Comm Lunar and Planet. Lab.*, **4**, 99 (No. 63).
Johnson, H. L., Coleman, I., Mitchell, R. I., and Steinmetz, D. L. 1968, *Comm. Lunar and Planet. Lab.*, **7**, 83.
Keenan, P. C. 1942, *Ap. J.*, **95**, 461.
———. 1963, in *Basic Astronomical Data*, ed. K. Aa. Strand (Chicago: University of Chicago Press), p. 78.
Kron, G. E. 1958, *Pub. A.S.P.*, **70**, 561.
Lee, T. A. 1968, *Ap. J.*, **152**, 913.
Low, F. J., and Johnson, H. L. 1964, *Ap. J.*, **139**, 1130.
Lynds, B. T. 1967, *Pub. A.S.P.*, **79**, 448.
McCammon, D., Münch, G., and Neugebauer, G. 1967, *Ap. J.*, **147**, 575.
McCuskey, S. W. 1967, *A.J.*, **72**, 1199.
Morgan, W. W., Whitford, A. E., and Code, A. D. 1953, *Ap. J.*, **118**, 318.
Nassau, J. J., Blanco, V. M., and Morgan, W. W. 1954, *Ap. J.*, **120**, 478.
Neckel, H. 1967, in *Interstellar Grains*, ed. J. Mazo Greenberg and T. P. Roark (NASA AP-140), p. 39.
Neckel, T. 1966, *Zs. f. Ap.*, **63**, 221.
Sharpless, S. 1956, *Ap. J.*, **124**, 342.
———. 1958, *Pub. A.S.P.*, **70**, 392.
———. 1965, in *Galactic Structure*, ed. A. Blaauw and M. Schmidt (Chicago: University of Chicago Press), p. 131.
———. 1966, *I.A.U. Symposium No. 24*, p. 345.
Starikova, G. A. 1960, *Soviet Astr.—AJ*, **4**, 451.
Stothers, R. 1969, *Ap. J.*, **155**, 935.
Stothers, R., and Chin, C. 1968, *Ap. J.*, **152**, 225.
———. 1969, *ibid.*, **158**, 1039.
Stothers, R., and Leung, K. 1970 (in preparation).
Sugimoto, D., Yamamoto, Y., Hōshi, R., and Hayashi, C. 1968, *Progr. Theoret. Phys.*, **39**, 1432.
Thompson, R. I., Schnopper, H. W., Mitchell, R. I., and Johnson, H. L. 1969, *Ap. J.* (*Letters*), **158**, L117.
Tsuji, T. 1966, in *Colloquium on Late Type Stars*, ed. M. Hack (Trieste), p. 260.
Vardya, M. S. 1966, in *Colloquium on Late Type Stars*, ed. M. Hack (Trieste), p. 242.
Walker, M. F. 1967, *Pub. A.S.P.*, **79**, 119.
Wawrukiewicz, A. S. 1970 (in preparation).
Weymann, R. J. 1962, *Ap. J.*, **136**, 844.
Wildey, R. L. 1964, *Ap. J. Suppl.*, **8**, 439 (No. 84).
Wildey, R. L., and Murray, B. C. 1964, *Ap. J.*, **139**, 435.
Woolf, N. J., Schwarzschild, M., and Rose, W. K. 1964, *Ap. J.*, **140**, 833.
Yamashita, Y. 1967, *Pub. Dom. Ap. Obs.*, **13**, 47.

© American Astronomical Society • Provided by the NASA Astrophysics Data System